

**NOVEL DESIGN OF ELECTRICAL MACHINE
FOR CEILING FAN**

By

HASNUL ZICKRY BIN HASHIM

Final Dissertation

A project dissertation submitted to the
Electrical and Electronics Engineering Programme

Universiti Teknologi PERTONAS

In partial fulfilment of the requirement for the

Bachelor of Engineering (Hons)

(Electrical & Electronics Engineering)

Universiti Teknologi Petronas

Bandar Seri Iskandar

31750 Tronoh

Perak Darul Ridzuan

Copyright of 2013

By

Hasnul Zickry Hashim, 2013

CERTIFICATION OF APPROVAL

Novel Design of Electrical Machine for Ceiling Fan

By

Hasnul Zickry Bin Hashim

A project dissertation submitted to the
Electrical and Electronics Engineering Programme

Universiti Teknologi PERTONAS

In partial fulfilment of the requirement for the

Bachelor of Engineering (Hons)

(Electrical & Electronics Engineering)

Approved by:

.....

(DR. TAIB IBRAHIM)

Project Supervisor

CERTIFICATION OF ORIGINALITY

I hereby verify that this report was written by me, Hasnul Zickry bin Hashim (11939). I am responsible for the work that I have submitted in this project. The procedures and results achieved throughout the project were conducted with my own effort except as specified in the reference and acknowledgement.

.....

(HASNUL ZICKRY HASHIM)

ABSTRACT

With the warm and humid climate throughout the year in Malaysia, ceiling fan has become an important electrical appliance for the cooling purpose in each house. The mechanical rotation of the existing ceiling fan is not fully utilised where the wasted kinetic energy from the blade rotation can be captured and converted into electricity. The purpose of this project is to propose a novel design of the electrical machine for the ceiling fan which capable in generating electricity. In this study, a permanent magnet machine configuration is selected in designing the ceiling fan model. Permanent magnet is small and compact with a higher and constant flux density resulted in higher torque and back electromotive force (EMF). This unique characteristic has make the permanent magnet machine suitable for both motor and generator purposes. Various literature studies had been conducted to study the effect of different configuration and variable parameter of the permanent magnet machine such as the number of poles and slot, slot angle, winding configuration and slot design towards its performance. Two new designs of the ceiling fan were proposed which consists of motor and generator fused into one system where the generated electricity will be used to provide power supply for other suitable household appliances. The design model will then be simulated and analysed by using finite element software, Ansoft Maxwell. The results were focused on the flux distribution and the back EMF of the system where the design is further optimised as the continuous improvement to achieve the best configuration of the ceiling fan machine.

TABLE OF CONTENTS

ABSTRACT	iv
CHAPTER 1: INTRODUCTION	1
1.0 Project Background.....	1
1.1 Problem Statement.....	5
1.2 Objective.....	5
1.3 Project Relevancy.....	6
1.4 Feasibility of the Project.....	6
CHAPTER 2: LITERATURE REVIEW	7
2.0 Introduction.....	7
2.1 Electrical Machine Type.....	7
2.2 Permanent Magnet Machine.....	8
2.3 Permanent Magnet Configuration.....	9
2.3.1 Slot angle.....	9
2.3.2 Number of Pole and Slot.....	10
2.3.3 Stator Winding.....	12
2.3.4 Slot Design.....	13
2.3.5 Notch and Reluctant Hole.....	14
2.3.6 Injected Stator Current.....	15
2.4 Conclusion.....	15
CHAPTER 3: METHODOLOGY	16
3.0 Introduction.....	16
3.1 Research Methodology.....	16
3.2 Process Flow.....	17
3.3 Gantt Chart.....	18
3.4 Tool.....	19
3.4.1 AutoCAD.....	19
3.4.2 Ansoft Maxwell.....	19
3.5 Conclusion.....	20
CHAPTER 4: PROPOSED DESIGN	21
4.0 Introduction.....	21
4.1 Design Consideration.....	21
4.2 Conceptual Design.....	22

4.3	Proposed Design	23
4.4	Conclusion	26
CHAPTER 5: RESULT AND DISCUSSION.....		27
5.0	Introduction.....	27
5.1	Simulation Design.....	27
5.2	Meshing Operation.....	28
5.3	Simulation Result.....	30
5.3.1	Flux Distribution.....	30
5.3.2	Air Gap Flux Density.....	35
5.3.3	Back EMF	37
5.4	Performance Analysis	40
5.5	Conclusion	43
CHAPTER 6: DESIGN OPTIMISATION.....		44
6.0	Introduction.....	44
6.1	Variation of Split Ratio.....	44
6.1.1	Optimisation Design	44
6.1.2	Optimisation Result	46
6.2	Variation of Pole Pitch Ratio	50
6.2.1	Optimisation Design	50
6.2.2	Optimisation Result	53
6.3	Conclusion	57
CHAPTER 7: CONCLUSION AND FUTURE WORK		58
7.0	Conclusion	58
7.1	Future Work.....	58
REFERENCES		59

LIST OF TABLES

Table 2.1	Comparison of electrical machine type.....	7
Table 3.1	Project Gantt chart and milestone	18
Table 3.2	List of software used for the project	21
Table 4.1	Consideration in designing the ceiling fan configuration.....	19
Table 4.2	Design parameter of the proposed design.....	25
Table 6.1	Variation of split ratio.....	46
Table 6.2	RMS value of induced voltage (split ratio).....	48
Table 6.3	Variation of pole pitch ratio.....	51
Table 6.4	RMS value of induced voltage (pole pitch ratio).....	55

LIST OF FIGURES

Figure 1.1	Electricity generation in Malaysia	1
Figure 1.2	Electricity consumption in Malaysia	2
Figure 1.3	Electricity Consumption per capita in Malaysia.....	2
Figure 1.4	Annual electricity consumption in Malaysia	3
Figure 1.5	Daily usage time of electrical appliance in Malaysia	4
Figure 2.1	Slot angle diagram of 8-pole 6-slot BLDC motor	9
Figure 2.2	The 12-pole 9-slot BLDC configuration.....	10
Figure 2.3	Variation of motor efficiency with number of poles	11
Figure 2.4	Output power from different pole number-constant slot number	11
Figure 2.5	Output power from different slot number-constant pole number	12
Figure 2.6	Winding configuration of 4-pole BLDC motor	12
Figure 2.7	Core shapes of 12-pole 9-slot BLDC motor	13
Figure 2.8	Rectangular notches on stator surface of a BLDC motor	14
Figure 2.9	Reluctant hole on stator tooth of a BLDC motor.....	14
Figure 2.10	Force ripple vs. induced current of 30-pole 5-slot BLDC motor.....	15
Figure 3.1	Project flow process	17
Figure 4.1	Design concept of novel ceiling fan.....	22
Figure 4.2	Proposed design A	24
Figure 4.3	Proposed design B.....	24
Figure 5.1	Modelled electrical machine	27
Figure 5.2	Modelled motor part	28
Figure 5.3	Modelled generator part.....	28
Figure 5.4	Meshed motor part and generator part	29
Figure 5.5	Meshed combined electrical machine	30
Figure 5.6	Open flux distribution of motor and generator part	30
Figure 5.7	Open flux distribution of electrical machine	31
Figure 5.8	Transient flux distribution of motor part	32
Figure 5.9	Transient flux distribution of generator part.....	33
Figure 5.10	Transient flux distribution of combined electrical machine	34
Figure 5.11	Arc line positioning in determining air gap flux density	35
Figure 5.12	Air gap flux density of motor part	36
Figure 5.13	Air gap flux density of generator part.....	36

Figure 5.14	Flux linkage of motor part	37
Figure 5.15	Induced voltage of motor winding	37
Figure 5.16	Flux linkage of generator part.....	38
Figure 5.17	Induced voltage of generator winding	39
Figure 5.18	Flux distribution of design A and B.....	40
Figure 5.19	Air gap flux density of design A and B (motor part).....	41
Figure 5.20	Air gap flux density of design A and B (generator part)	41
Figure 5.21	Induced voltage of design A and B (motor part)	42
Figure 5.22	Induced voltage of design A and B (generator part).....	42
Figure 6.1	Design split ratio	44
Figure 6.2	Design with split variation	45
Figure 6.3	Air gap flux density of S1, S2, S3, S4 and S5 (motor part).....	46
Figure 6.4	Air gap flux density of S1, S2, S3, S4 and S5 (generator part)	47
Figure 6.5	Induced voltage of variation S1, S2, S3, S4 and S5 (motor part)	47
Figure 6.6	Induced voltage of variation S1, S2, S3, S4 and S5 (generator part) ..	48
Figure 6.7	Performance plot of split ratio optimisation	49
Figure 6.8	Design pole pitch ratio	51
Figure 6.9	Design with pole pitch variation	52
Figure 6.10	Air gap flux density of P1, P2, P3, P4 and P5 (motor part).....	53
Figure 6.11	Air gap flux density of P1, P2, P3, P4 and P5 (generator part)	53
Figure 6.12	Induced voltage of variation P1, P2, P3, P4 and P5 (motor part)	54
Figure 6.13	Induced voltage of variation P1, P2, P3, P4 and P5 (generator part) ..	55
Figure 6.14	Performance plot of pole pitch ratio optimisation	55

CHAPTER 1

INTRODUCTION

1.0 Project Background

The advance development in science and technology nowadays has allow us to convert electrical energy into other desired energy form such as mechanical, thermal, luminous, sound and more. Therefore, electrical energy has been placed as one of the most vital form of energy in our modern world. The key factor for the survival of most industrial and domestic sectors nowadays is the efficiency in managing the electricity consumption. In addition, the development level of a country nowadays is determined by the average electrical energy consumption by each citizen (per capita).

Realising the importance of the electricity towards the development and advancement of the country, Malaysian government had decide to increase the generation of the electricity of the country. Figure 1.1 shows the increasing amount of electricity being generated in Malaysia from year 2000 until 2011 [1]. Meanwhile the following Figure 1.2 and Figure 1.3 show the amount of electricity consumption and consumption per capita in Malaysia respectively for the same range of year [1].

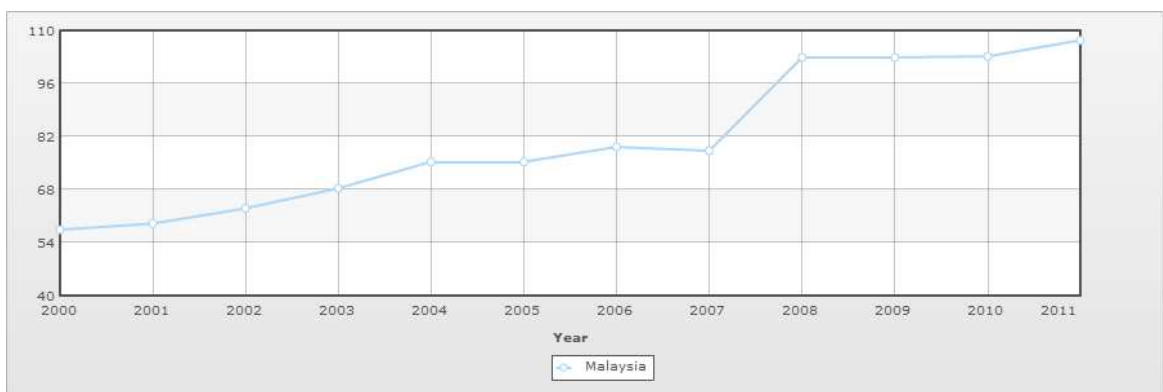


Figure 1.1: Electricity generation in Malaysia (billion kWh) [1]



Figure 1.2: Electricity consumption in Malaysia (billion kWh) [1]

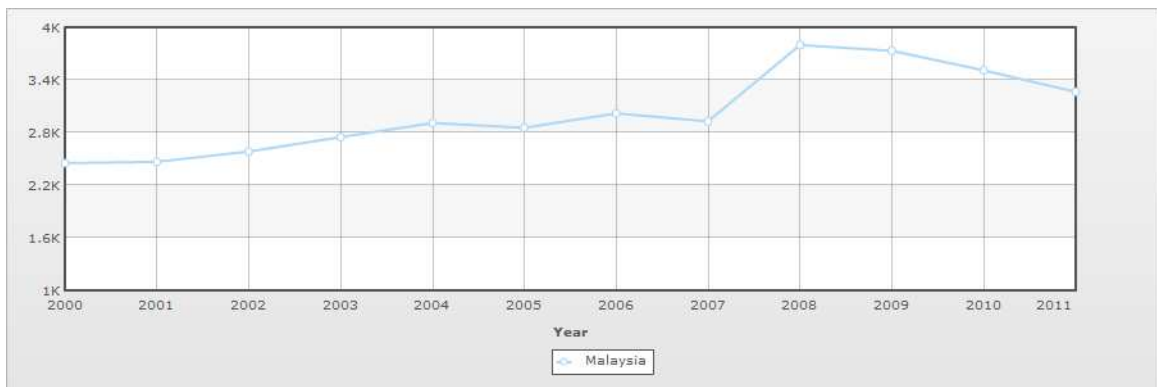


Figure 1.3: Electricity consumption per capita in Malaysia (kWh per person) [1]

Based from the graphs above, electrical energy consumption in Malaysia had started to decrease starting from year 2010 despite the increasing energy generation of the country and predicted to continue decreasing for year 2012 and onwards. The decrement trend of the energy consumption is high possibility due to the improved efficiency of the electrical appliance nowadays in minimising the power rating consumption as much as possible.

With the costs of the energy that continuously increasing all over the world, people are now looking for the options where they can reduce the power consumption in their daily used electrical appliances and utilities so that they can cut off some of the expenditure money spent on the electrical bill. In this study, the scope will be focused on the ceiling fan.

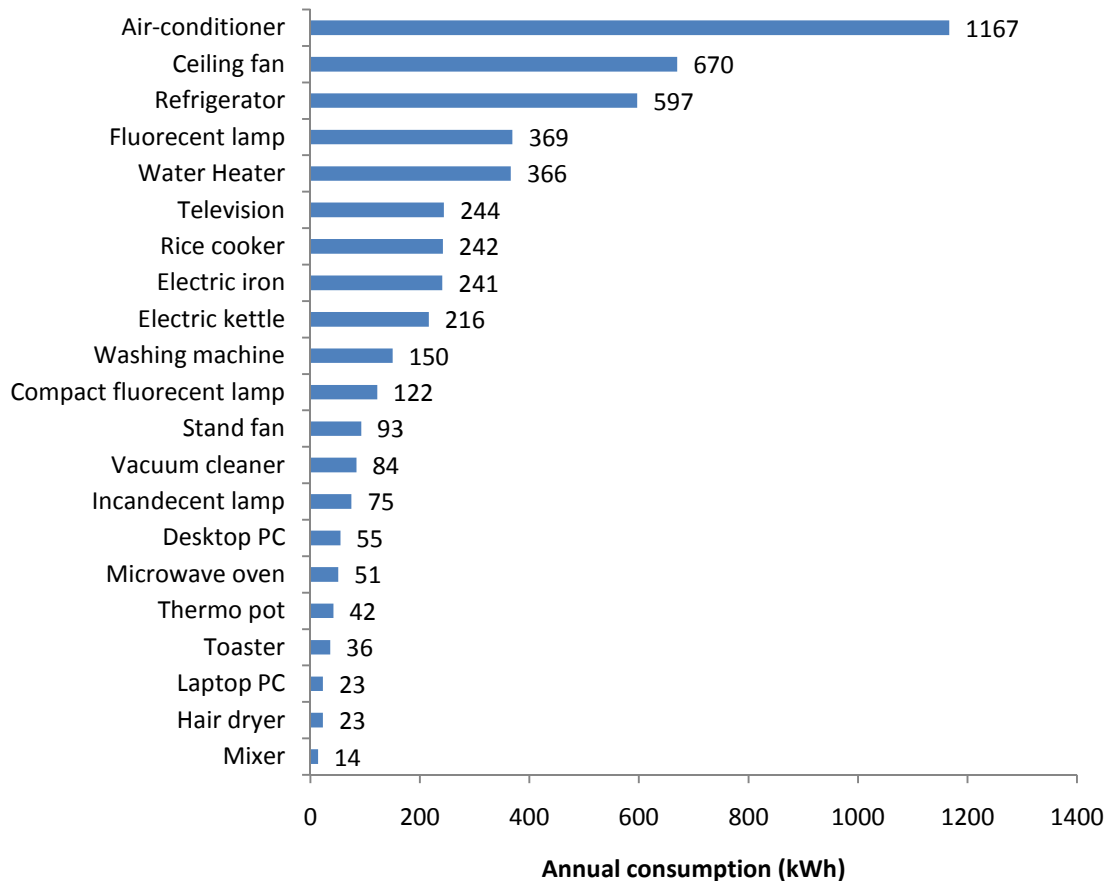


Figure 1.4: Annual electricity consumption in Malaysia [2]

Figure 1.4 shows annual electricity consumption of various household electrical appliances in Malaysia [2]. Considering the country's climate that warm and humid throughout the year, about 30 percent of the energy consumptions are coming from cooling appliances such as air-conditioner, ceiling fan and stand fan. Among these three electrical appliances, ceiling fan is ranked in second place as the most energy-consuming appliance throughout the year which consumes about 10 percent of the total annual energy consumption.

Along with the power ratings that are varies for each electrical appliance which correspond to the amount of energy that is being consumed, the energy consumption also being affected by the usage time of that appliance. This means the longer time the appliance being used, the more energy being consumed. Figure 1.5 shows the graph of daily usage time of the same electrical appliance as in Figure 1.4 [2].

The time usage of each electrical appliance is subjective and may varies for each house, depending on the requirement and the need of its user. From Figure 1.5, the

average daily usage time for the ceiling fan in Malaysia is 8 hours, considering the ceiling fan only being operated when there are presence of people inside the house [2]. The time range where the ceiling fan being fully optimised is between 6 p.m. to 12 a.m. since most the houses are not being occupied during the day due to people leave for work.

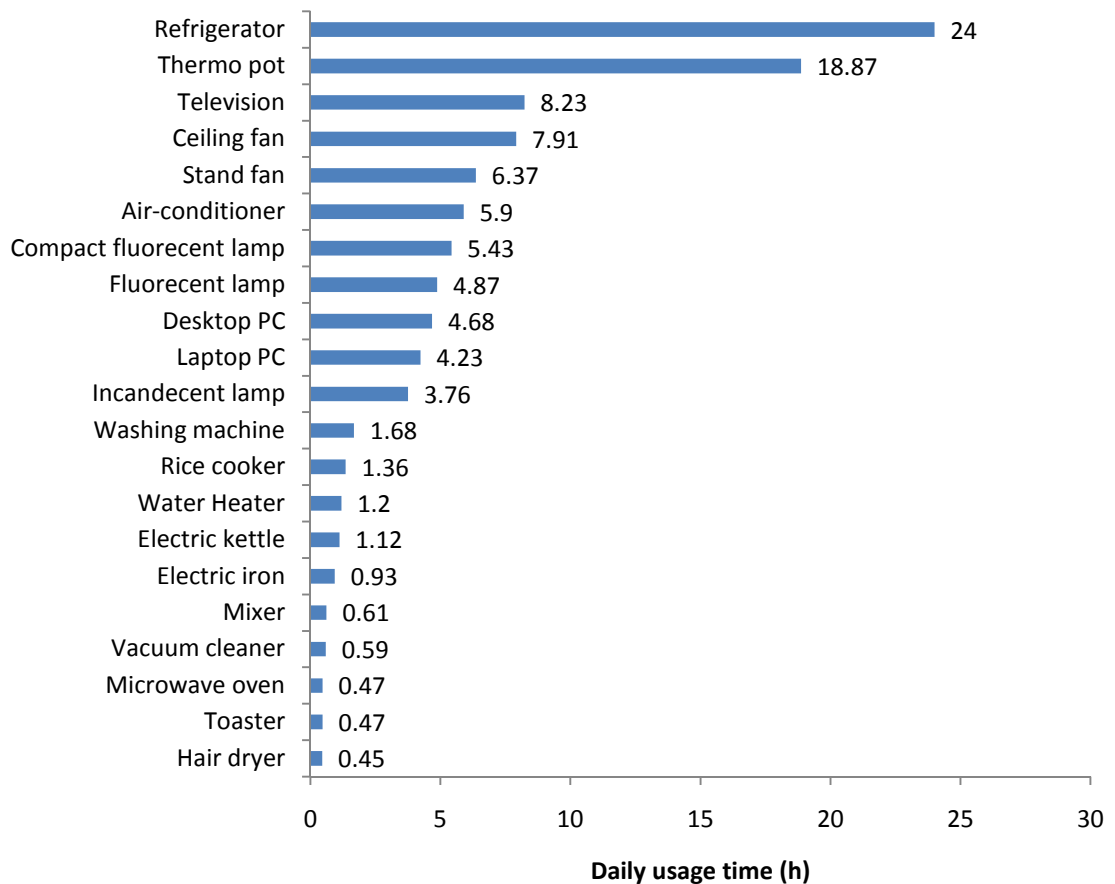


Figure 1.5: Daily usage time of electrical appliance in Malaysia [2]

People tend to compare ceiling fan with air-conditioner. Air-conditioner seems to be the most favourable cooling appliance since it provides faster cooling time and higher comfort level. However, air conditioner consumes more electrical energy compared to ceiling fan and requires higher maintenance cost. Because of that, not many people could afford to have air-conditioner in their house thus preferring ceiling fan as the main cooling appliances and air-conditioner as the additional cooling appliance which depends on individual affordability.

1.1 Problem Statement

With the climate condition of Malaysia which is constantly warm and humid throughout the year, ceiling fan had become one of the importance cooling appliances for almost every house in Malaysia. A conventional ceiling fan is typically uses a single-phase induction motor. The drawback with the low-cost single-phase induction motor are low power factor, low efficiency and poor pulsating torque, thus resulted in a poor performance of the machine. In addition, the existing ceiling fan is not fully utilised where the kinetic energy resulted from the rotation of the ceiling fan motor can actually be captured to generate electricity.

1.2 Objective

The main objective of this project is to propose a novel design of the electrical machine for the ceiling fan by using permanent magnet configuration which capable in generating electricity for other suitable appliance. The other sub-objectives are:

- i. To conduct literature review on permanent magnet machine and various parameter of the motor that lead in obtaining the best design configuration.
- ii. To propose new designs of ceiling fan system which consists of motor and generator combined into one system.
- iii. To simulate the proposed design by using finite element method in analysing the outcome result.
- iv. To optimise the design to obtain the optimum performance of the system.

1.3 Project Relevancy

This project acquires the knowledge and application of electrical and electronics field of study especially in electrical machine as the design of the ceiling fan is mostly dealing with both motor and generator. The knowledge in using the finite element software, Ansoft Maxwell is also necessary in simulating the proposed design model to study the outcome results such as flux distribution and back EMF. Besides, this project fully applies a standard problem solving approach in optimising the design of the ceiling fan model. This project involve lots of engineering discipline which certainly relevant to the purpose of this final year project

1.4 Feasibility of the Project

The project will be conducted in two semesters which include three major phases; design, simulation and optimisation of the ceiling fan model. The first semester will be focused on proposing new design models of the novel ceiling fan and performing the design simulation by using finite element software. The following semester will be focused on the design optimisation to obtain the best configuration of the model. The objective is to design and model a novel design of ceiling fan system that can generate electricity for other suitable appliances. Finite element software, Ansoft Maxwell which is available in the university facility will be used to simulate the design of the ceiling fan to study the back EMF and the magnetic flux distribution of the new system. Therefore, this project is feasible to be completed within the time frame.

CHAPTER 2

LITERATURE REVIEW

2.0 Introduction

In order to design the electrical machine for the ceiling fan, various literature reviews of past studies need to be conducted in order to produce a good machine design. Different types of electrical machines will be studied and compared to select the best machine type which will be used for the novel ceiling fan system. Various design configurations of the selected electrical machine will be studied focusing in obtaining higher output power and minimum cogging torque

2.1 Electrical Machine Type

There are various type of electrical machine that can be used for the ceiling fan system such as induction machine, synchronous machine, direct current machine and permanent magnet machine. Each type of the machine has their advantages and disadvantages. Table 2.1 show the comparison of the electrical machine in term of the performance and feasibility for the ceiling fan application.

Table 2.1: Comparison of electrical machine type

Machine Type	Advantage/Disadvantage
Induction machine	Advantage: Simpler, cheaper cost, no brushes, rugged, suitable for heavy load Disadvantage: Poor starting torque, lagging power factor, need high start-up current
Synchronous machine	Advantage: Operate at constant speed, adjustable power factor, high efficiency at low speed Disadvantage: Require external dc source, require no load before start-up, may require brushes
DC machine	Advantage: Low cost, high starting torque, suitable for traction/towing power Disadvantage: Brushes cause friction and spark, require load before start-up

Permanent magnet machine	<p>Advantage: Higher power and torque density, smaller and compact, do not required current for excitation field, suitable for low load application</p> <p>Disadvantage: Expensive magnet, weight increased with size, high cogging torque</p>
--------------------------	--

From the comparison, the criteria of permanent magnet are suitable for the purpose of rotating the machine as well as generating the electricity. Therefore we will focus on utilising the permanent magnet machine in designing the novel design of the ceiling fan.

2.2 Permanent Magnet Machine

Magnetism is one of the most important elements in the study of electricity. By manipulating the knowledge of magnetic field, two types of energy can be produced; mechanical energy and electrical energy. Generator converts mechanical energy into electrical energy while motor converts electrical energy into mechanical energy and both of the energy can be generated either by using linear or rotary movement.

Most of the electrical machines nowadays use the application of the permanent magnet technology. Permanent magnet motor contributes in a wide range of power application ranging from mW to hundreds kW thus covering a wide variety of application fields including industrial sector, domestic life, automobile and transportation, defence force, aerospace, healthcare equipment, power tool, renewable energy systems and more [3].

Permanent magnet machine provides a higher power and torque density and is better than other electromagnetically-excited machine in term of its dynamic performance due to the constant and higher magnetic flux density generated by the magnet itself. Besides, there is no additional current needed to produce the excitation field thus increasing the efficiency of the machine. The manufacturing and maintenance of the permanent magnet is simple which make it suitable for mass production purposes [3].

The side effect of using permanent magnet as the rotor is mostly related to cogging torque produced by the machine due to the interaction between the rotor's permanent magnet and stator's slot teeth. This cogging torque gave unfavourable effect to the performance of the motor as well as creating unwanted vibration and noise [4].

2.3 Permanent Magnet Configuration

Various studies had been conducted over the few past decades in order to fully optimise the permanent magnet machine as well as resolving the problem of high cogging torque resulted from the permanent magnet. Some variable parameters of the machine are adjusted and attuned to study the effect on the machine performance in determining the best configuration of the permanent magnet machine. Some of the investigated parameter studied in this literature review includes the slot angle, number of pole and slot, stator winding, slot design, notch and reluctant holes and injected stator current.

2.3.1 Slot Angle

The angle gap between the stator slots affects the performance of the permanent magnet motor. Taeyong Y. [5] had conducted an analysis on the effect of cogging torque and magnetic forces as the slot angle changes in an exterior rotor type permanent magnet motor. The motor as shown in Figure 2.1 is used for the high-RPM application of the hard disk drive and have a configuration of 8-pole and 6-slot. The result conclude that the optimum slot angle obtained produce minimum cogging torque but the angle is not optimum in reducing the magnetic force.

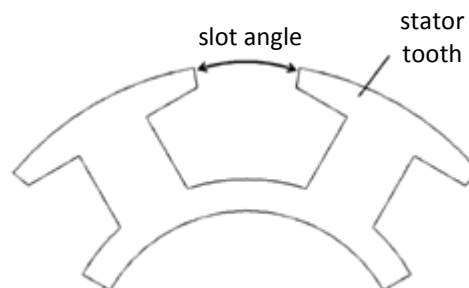


Figure 2.1: Slot angle diagram of 8-pole 6-slot BLDC motor [5]

Another study was done by Chen S.X. et al [6] to study the effect of the same parameter of slot angle in reducing the cogging torque of the motor. The motor that is used for the application of CD-ROM spindle have a configuration of 12-poles and 9-slot as illustrated in Figure 2.2. From the result, the optimum slot angle obtained is proved to be able to produce minimum cogging torque and noise-to-signal (N/S) ratio but is not optimum in maximising the running torque of the motor. The angle between

the slots for both studies is reasonably small to produce a minimum cogging torque and this angle may vary for different configuration, depending on the other parameter of the motor such as the number of pole and stator as well as the motor diameter.

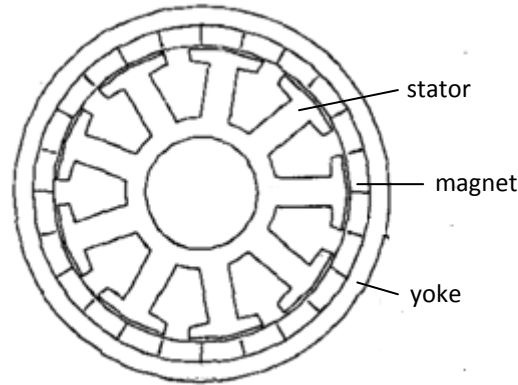


Figure 2.2: The 12-pole 9-slot BLDC configuration [6]

2.3.2 Number of Pole and Slot

The efficiency and the cogging torque of the permanent magnet motor also affected by the number of pole and slot inside the machine. Based on the study done by Fazil M. and Rajagopal K.R. [7] on the pole configuration of the permanent magnet BLDC ceiling fan, the result shows that the efficiency of the motor increase with the number of pole. Figure 2.3 show the analysis result of the motor efficiency with the variation of the pole number.

The higher pole number provides the better efficiency of the motor. However, higher number of pole and stator requires a high manufacturing cost which is not suit for a mass production of the electrical machine. Therefore, a wise consideration is needed in determining the optimum number of pole and slot to balance between the machine performance and the ease of the manufacturing.

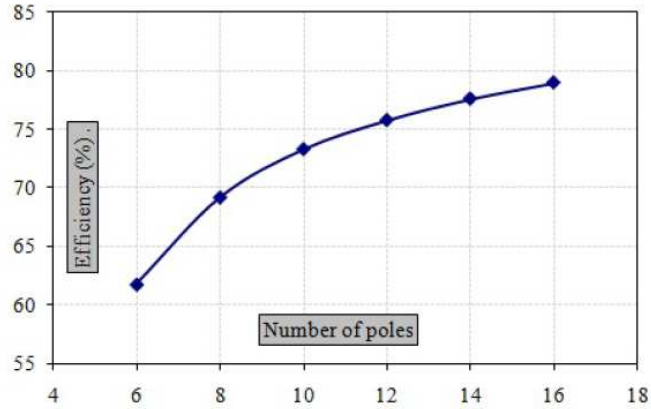


Figure 2.3: Variation of motor efficiency with number of poles [7]

Another similar study had been conducted by Yue Zhang et al [8] to show how the number of pole and slot can affect the performance of the permanent magnet machine in different application. The study is focused on a direct-driven permanent magnet wind generator to find the optimum pole-slot number configuration for the machine. Based on the results shown from Figure 2.4 and Figure 2.5, the combination of pole and slot number which produce the smallest slot/pole ratio will produce a higher output power.

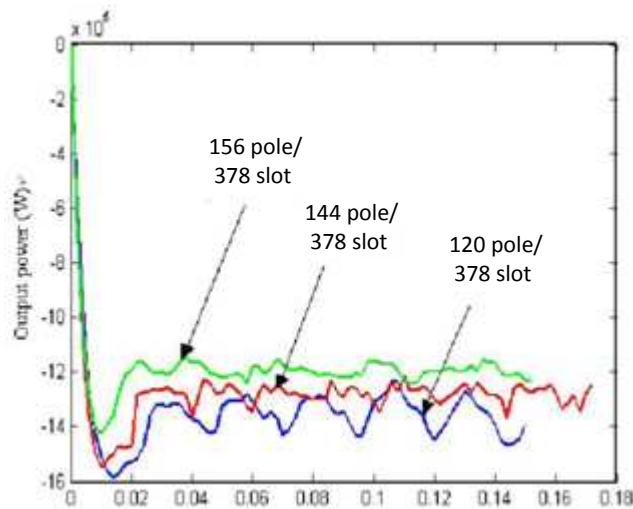


Figure 2.4: Output power from different pole number with constant slot number [8]

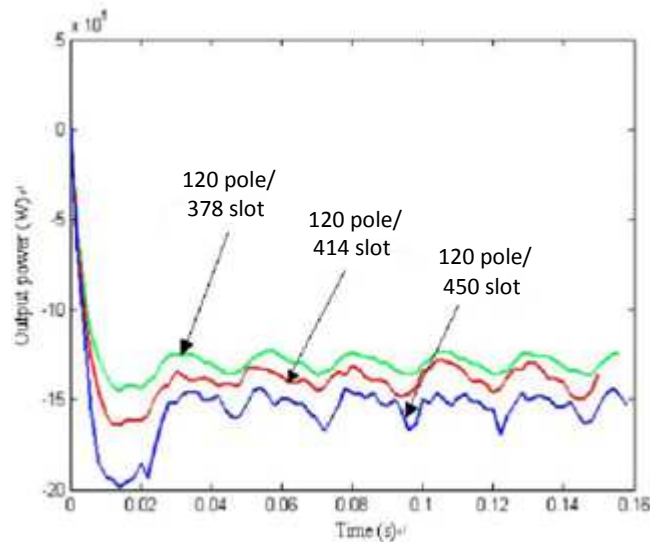


Figure 2.5: Output power from different slot number with constant pole number [8]

2.3.3 Stator Winding

The winding configuration of the stator slot also affects the performance of the motor in term of its cogging torque and winding factor. Three different winding configurations of 4-pole internal rotor which have distributed winding (a), single-layer concentrated winding (b) and double-concentrated winding (c) as shown in Figure 2.6 had been studied by Magnussen F. and Sadarangani C. [9] to analyse the performance of the permanent magnet machine.

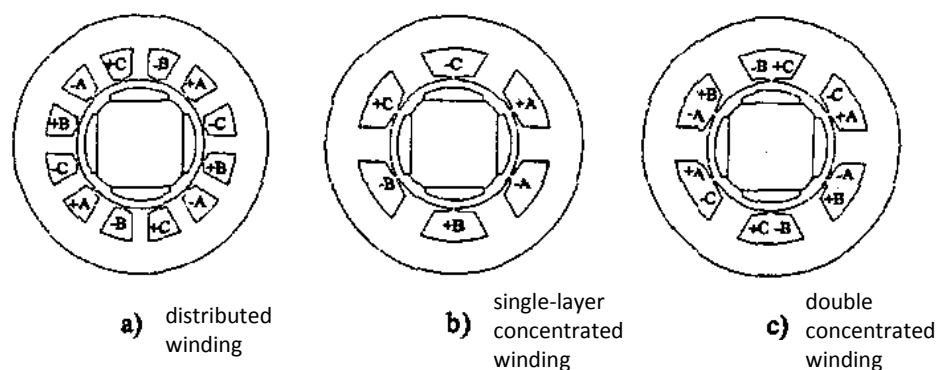


Figure 2.6: Winding configuration of 4-pole BLDC motor [9]

Based from the result of the analysis, concentrated winding would have advantage by required only two-third of the total pole pitch length for its slot pitch. However, concentrated winding configuration will lead to a poor winding factor as compared to distributed winding configuration which having ideal winding factor of 1. However,

with the better combination of the number of pole and slot of the concentrated winding configuration, a higher winding factor and lower cogging torque can be achieved.

2.3.4 Slot Design

Ki-Jin Han et al [10] had done the analysis on the effect of the core shape of the stator towards the performance of the motor in term of its cogging torque. Figure 2.7 shows four different designs of the core shapes of the stator which are basic core (a), grooved core (b), rounded core (c) and optimal core (d). The analysis had proved that both rounded and optimal core are better in reducing the cogging torque as much as 90% as compared to the basic core.

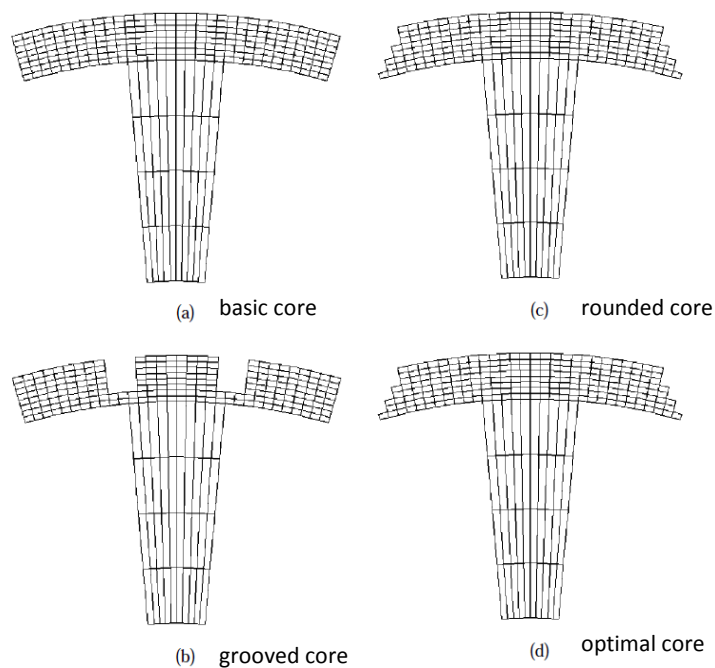


Figure 2.7: Core shapes of 12-pole 9-slot BLDC motor [10]

2.3.5 Notch and Reluctant Hole

Cogging torque can be reduced by providing a constant air gap energy between the stator and rotor. Study done by Chung T.K. [11] shows that by placing two small rectangular notches on each tooth surface as illustrated in Figure 2.8 can reduce the cogging torque of the permanent magnet motor. As the notches might be helpful in reducing the cogging torque, it had produced a negative side effect on the demagnetization margin as well as the performance of the motor due to the rough surface of the stator tooth. [12].

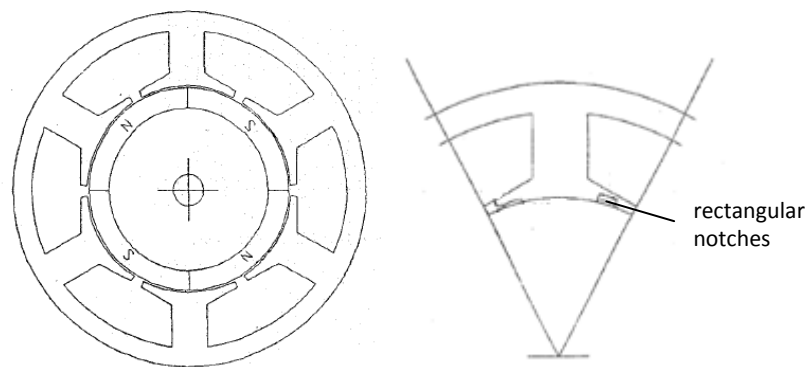


Figure 2.8: Rectangular notches on stator surface of a BLDC motor [11]

To further improve the motor performance, Gizaw D.[12] had proposed a new stator configuration for the electrical machine. Figure 2.9 shows the new configuration proposed where the notches on the stator tooth were being replaced by reluctant holes. Reluctant hole carries the same function as the notches in reducing the cogging torque but allows a smooth surface of the pole and improves the motor demagnetisation margin.

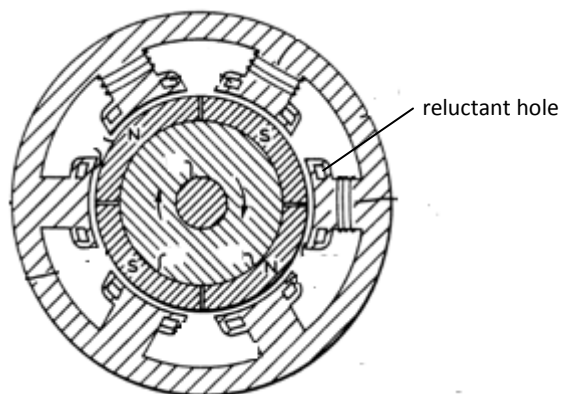


Figure 2.9: Reluctant hole on stator tooth of a BLDC motor [12]

2.3.6 Injected Stator Current

In a permanent magnet motor, the turning force of the motor is being influenced by the strength of flux field of the permanent magnet and the injected current on the stator of the motor. By weakening the field strength of the commutated BLDC motor which can be achieved by reducing the injected current to the stator winding, the radial force and the acoustic noise produced can be reduced [13]. Figure 2.10 shows the result obtained by Jiao G. et al [13] where the force ripple of the motor can be reduced by reducing the injected current.

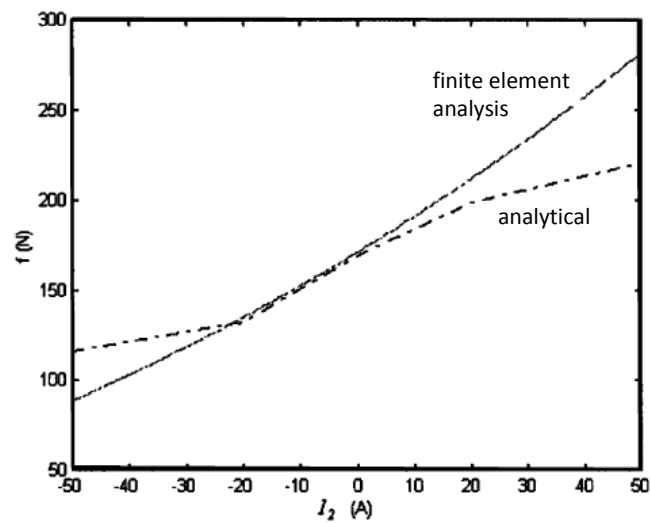


Figure 2.10: Force ripple, f versus induced current, I of 30-pole 5-slot BLDC motor [13]

2.4 Conclusion

Based from the conducted literature review, permanent magnet machine is selected to be used in designing the novel ceiling fan system. Various design configurations of the permanent magnet machine such as slot angle, pole and slot ratio, stator winding, slot design, reluctant holes and injected stator current had been studied to find the configuration of design which produces higher power output and minimum cogging torque. These will become a guideline in designing the mechanism of the ceiling fan system which will be discussed in Chapter 4.

CHAPTER 3

METHODOLOGY

3.0 Introduction

In order to achieve the objectives of the case studies within the allocated time, the establishment of a specific framework need to be created. A good planning and scheduling on a project will greatly influence the outcome of the conducted project. This chapter will discuss the research methodology of the case studies. The process flow the project and tools will be defined.

3.1 Research Methodology

In order to achieve the main objective of this project, the goals for the four sub objectives which had been discussed earlier needed to be accomplished. In designing the electrical machine for the ceiling fan, detailed literature review on the selected paper will be focused on the permanent magnet machine configuration. The factors which affect the performance of the permanent magnet motor also will be taken into account in order to find the best machine configuration.

For the second sub objective which is proposing a new design of ceiling fan system, a good consideration and justification need to be conducted before designing the ceiling fan model. This is to ensure the model designed is suitable for mass production and meet the current market demand.

For the third sub objective, the proposed design model later will be simulated by using finite element software which is available in the lab. The outcome result of the ceiling fan design will be study in term of its performance and efficiency. The back EMF and the flux distribution of the machine will be analysed.

For the last sub objective, after gathering the analysis result of the proposed model design, the model will then be fine-tuned and adjusted to further optimise the design configuration and will be analysed by using the same method of finite element analysis.

3.2 Process Flow

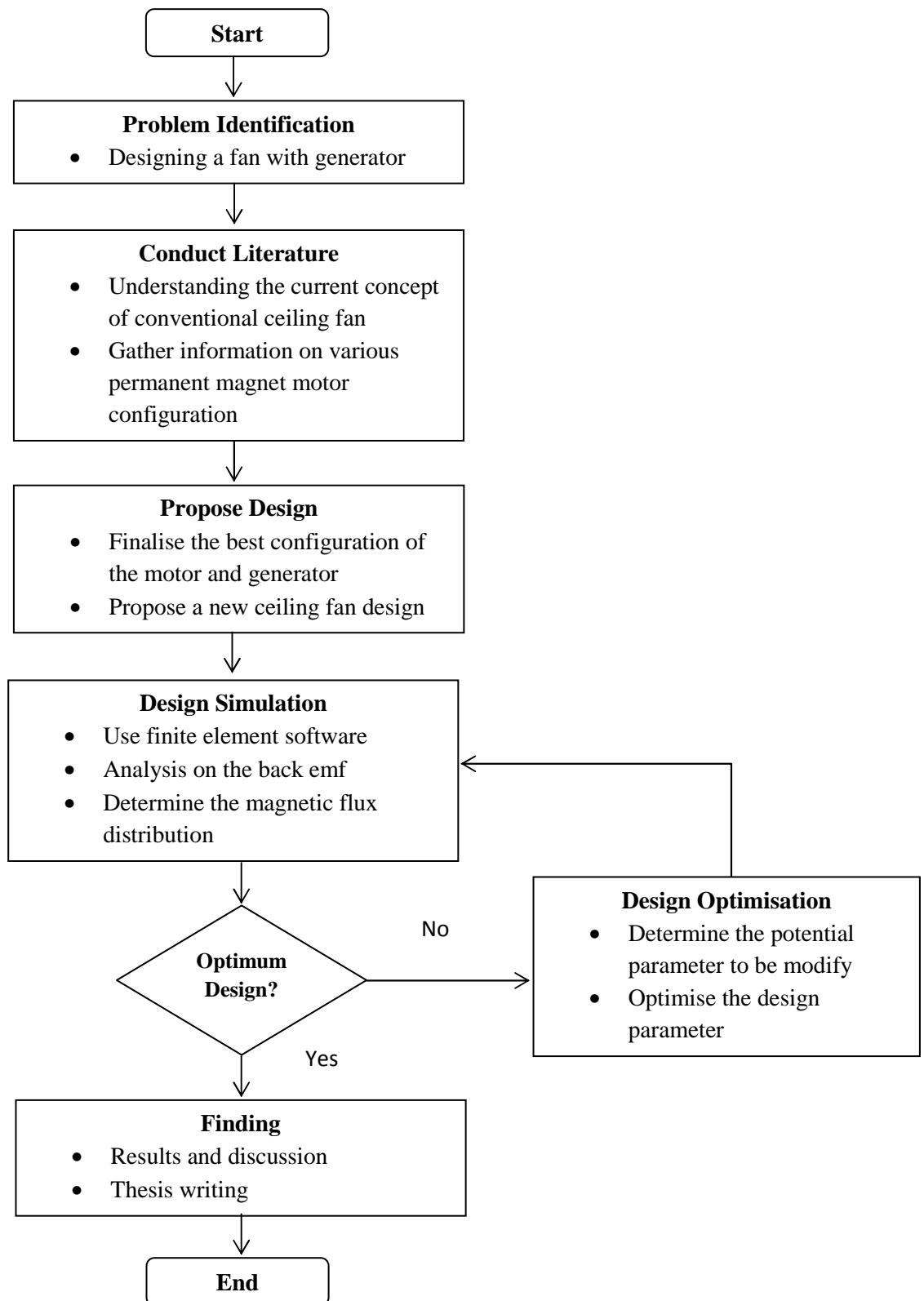


Figure 3.1: Project flow process

3.3 Gantt Chart

Table 3.1: Gantt chart and milestone for the project

No	Detail/ Milestone	1	2	3	4	5	6	7	8	9	10	11	12	13	14
FYP 1															
1.	Topic selection														
2.	Purpose understanding														
3.	Conduct literature review														
4.	Extended proposal submission (27/6)														
5.	Design the proposed model														
6.	Proposal defend (4/7-11/7)														
7.	Simulate the proposed design														
8.	Analyse the result outcome														
9.	Draft report submission (10/8)														
10.	Interim report submission (15/8)														
FYP 2															
11.	Design the model optimisation														
12.	Simulate the optimisation model														
13.	Progress report submission (5/11)														
14.	Analyse the result outcome														
15.	Electrex (28/11)														
16.	Draft report submission (7/12)														
17.	Final Report submission (14/12)														
18.	Technical paper submission (14/12)														
19.	Viva presentation (20/12-21/12)														
20.	Hardbound submission (7/1)														

3.4 Tool

Table 3.2: List of software used for the project

No	Software	Purpose
1.	Microsoft Visio	To design the electrical machine configuration
2.	AutoCAD	To design the electrical machine of the model
3.	Ansoft Maxwell	To simulate analyse the proposed design model
4.	Microsoft Excel	To tabulate result data
5.	Microsoft Word	To writing the report

3.4.1 *AutoCAD*

AutoCAD is a universally known software used by the engineer and designer for 2D and 3D design, modelling and architectural drawing. AutoCAD is user-friendly software that allows the designer to design a drawing model ranging from a simple design to complex design. Precise measurement of length and angle helps the designer to realise the design into 3D design. AutoCAD is one of the powerful tools for the engineer where the drawn design can be exported to other software such as Ansoft Maxwell for further analysis of the design.

3.4.2 *Ansoft Maxwell*

Ansys software is one of the finite element analyses (FEA) software that is widely used in engineering field which involves the task of designing and analysing a 3D and 2D electromagnetic and electromechanical model such as motor, transformers, actuator and sensor [14]. Ansoft Maxwell is one of the applications of Ansys software which specialise in electrical machine simulation. This simulation software allows the designer to build electrical machine model and perform test analysis to study the magnetostatic, electrostatic and transient behaviour of the designed model. By using the meshing application of the software, flux distribution as well as the back EMF for the rotary and linear machine can be simulated thus giving flexibility to the designer to update the parameter and configuration of the model design.

3.5 Conclusion

In this chapter, the research methodology of the case study is defined. There are four stages on how the case studies will be performed; conduct literature review on various design configuration of the ceiling fan, propose new ceiling fan designs, carry out the simulation for the proposed design and perform design optimisation. The project flow chart as well as the related Gantt chart is created in order to achieve the objectives of the case study within the timeframe. Tools which will be used throughout the case studies also will be defined.

CHAPTER 4

PROPOSED DESIGN

4.0 Introduction

Based on the literature review discussed in Chapter 2, there are many factors which affect the performance of the permanent magnet machine such as the number of pole and slot, slot angle, stator winding and others. This chapter will discuss on the design mechanism of the ceiling fan including the operational idea and the proposed design of the machine.

4.1 Design Consideration

The main objective of this project is to propose a novel design of the permanent magnet ceiling fan system which can generate electricity. Therefore, some initial design considerations are needed in designing the system. The Table 4.1 below show the justification in designing the ceiling fan system.

Table 4.1: Consideration in designing the ceiling fan configuration

Consideration	Justification
Reduce cogging torque	Cogging torque produce unwanted noise and mechanical vibration in the system that will cause discomfort and lead to short lifespan of the machine. The design configuration of the system need to provide cogging torque as low as possible to reduce this unwanted noise and vibration.
Easy to manufacture	Some complex design configuration may result in better performance from the machine but is difficult to manufacture. Since the ceiling fan system is design for the mass production system, the configuration of the system need to be simple and easy to be manufactured.
High force capability	The better high force capability of the system, the better the machine. The capability performance of the ceiling fan machine need to be balance with the power requirement and the system proficiency.

Back EMF	Back electromotive force (EMF) is force produced from the spinning of the armature rotor of the system. Back EMF increase the apparent resistance of the system thus consumes less power and increase the efficiency of the system
----------	--

4.2 Conceptual Design

Figure 4.1 shows the basic idea of the ceiling fan model which will be used in designing the configuration of the ceiling fan system. The ceiling fan will use permanent magnet configuration as the permanent magnet have constant and higher magnetic flux density which suitable for both application of motor and generation. The new novel design for the ceiling fan consists of two parts; motor and generator.

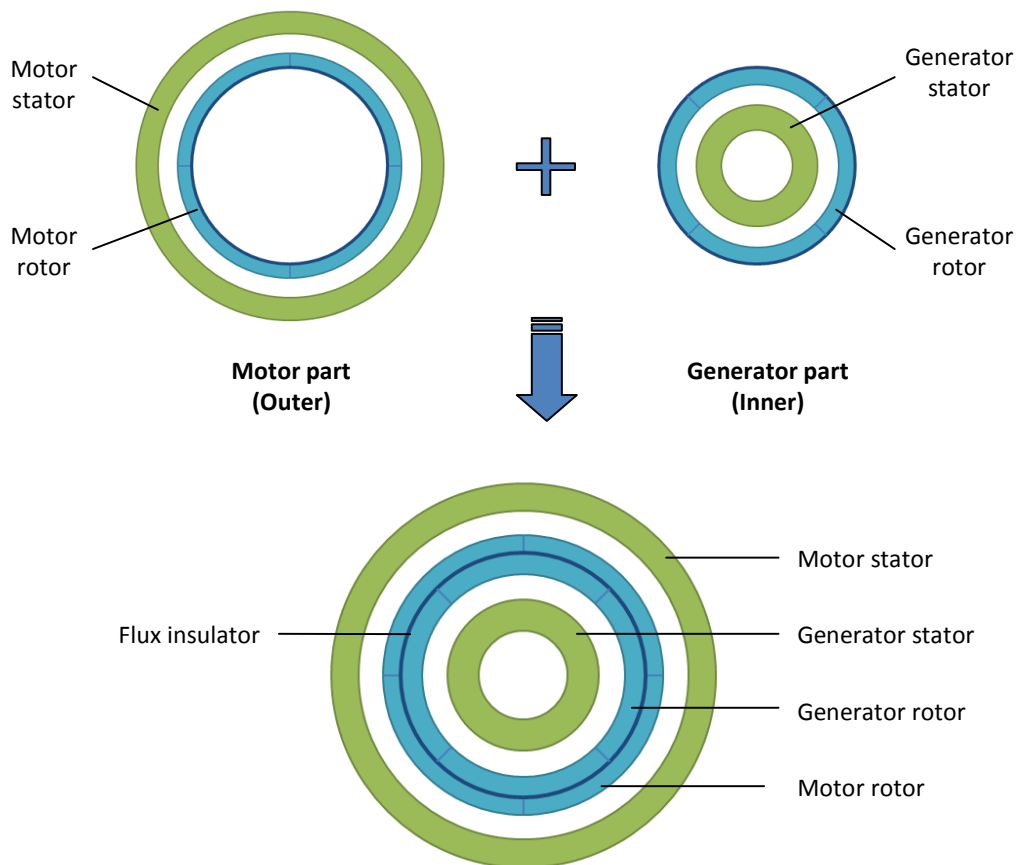


Figure 4.1: Design concept of the novel ceiling fan

The motor part of the ceiling fan carries the normal function of the conventional ceiling fan where it will feed the electricity from the main power source and will then be channelled into the stator winding of the motor. The magnetic flux will be generated as the current flow into the winding of the stator and causes the permanent magnet rotor part in the middle section of the machine to rotate based on the principle of normal permanent magnet motor. In this case, the electrical energy will be converted into kinetic energy.

The rotor part of the motor will be attached with the generator rotor inside. As the rotor of the motor rotates, the inner rotor will rotate simultaneously which will act as the generator. The rotating inner permanent magnet rotor will then will induce current in the winding coil of the generator part and thus generates electricity. In this case, the kinetic energy from the rotor movement will be captured and converted into electrical energy. The electrical energy generated will be used for other suitable electrical appliances.

To avoid any magnetic flux interference from both parts, the motor rotor and generator rotor will be separated by the aluminium sheet. Aluminium element acts as a good magnetic flux insulation to prevent magnetic flux leakage.

4.3 Proposed Design

Considering the cogging torque and the manufacturing cost issues raised by permanent magnet machine, two new designs are proposed such that these new models are capable in generating electricity with relatively low cogging torque and manufacturing cost. The designs were created by using AutoCAD software which employing the actual dimension of the model design.

Figure 4.2 and Figure 4.3 show two different construction of the proposed electrical machine design of the ceiling fan. The rotor for both motor and generator parts of the machine consist of ferrite permanent magnet where both of the rotors are attached together as one moving part, separated by a thin aluminium sheet in between which acts as the magnetic flux separator. Permanent magnet does not require a complicated installation as compared to other type of electrical machine and quite light for low load application.

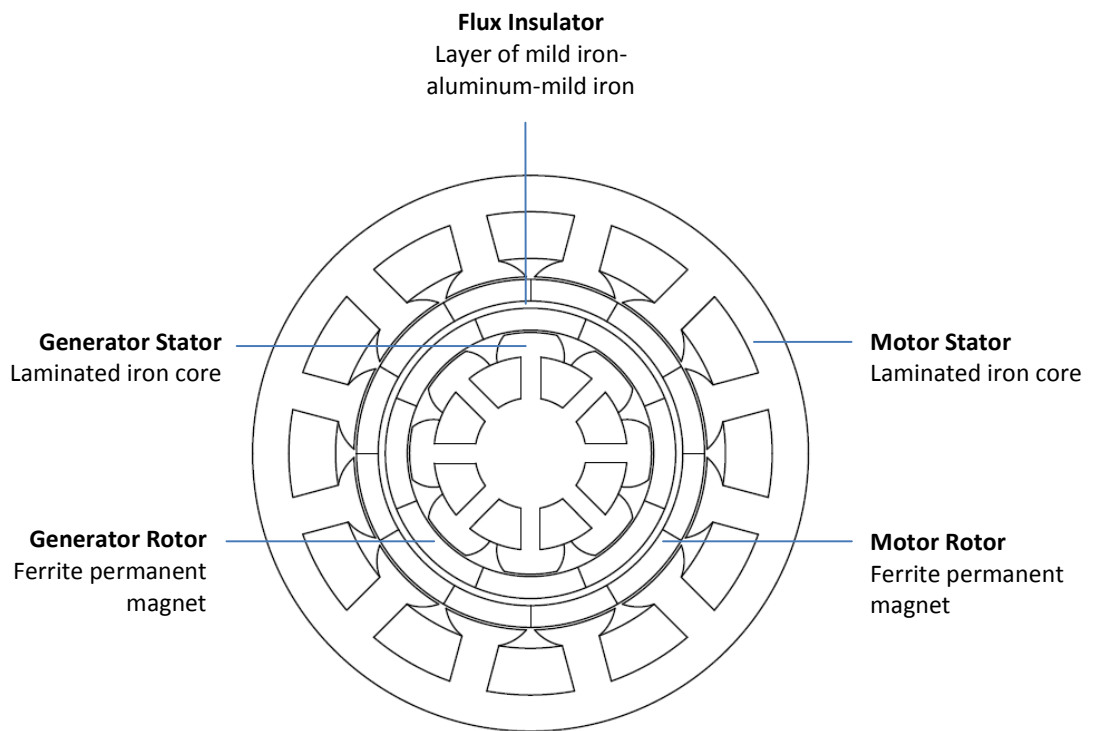


Figure 4.2: Proposed design A

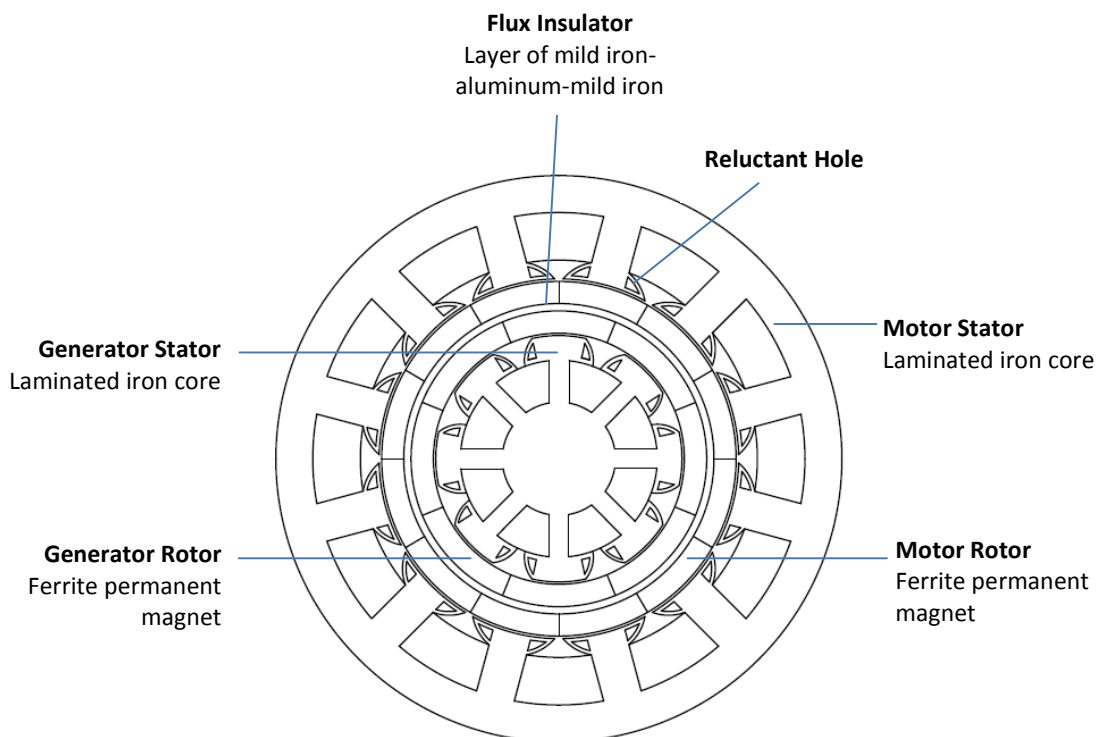


Figure 4.3: Proposed design B

The stator part for both motor and generator consist of laminated iron core designed to reduce the eddy current in the machine. A set of copper coil winding will be fitted on the stator tooth of both motor and generator to serve different two purposes; to supply moving power to the motor and to harvest the energy from the rotating rotor respectively. Design A and B both are having almost the same design parameter and configuration except that Design B has reluctant holes drilled on the tooth of its stator, functioning in reducing the cogging torque of the machine.

Table 4.2 shows the tabulated design parameter for both ceiling fan designs.

Table 4.2: Design parameter of the proposed design

Parameters	Dimension (mm)
Aluminium sheet	3
Motor (outer part)	
Back iron thickness	15
Stator outer diameter	230
Stator inner diameter	146
Number of pole/slot	6/12
Slot angle	2
Air gap	1
Permanent magnet thickness	9
Stator tooth length	27
Stator tooth width	15.8
Number of coil turns	250
Generator (inner part)	
Stator outer diameter	100
Number of pole/slot	4/8
Slot angle	5
Air gap	1
Permanent magnet thickness	9
Stator tooth length	27
Stator tooth width	8.35
Number of coil turns	250

The design parameter shown will be used to create the model drawing of design A and B. Then the finish drawing will be exported into the Ansoft Maxwell for the design simulation which will be further discussed in the next chapter. Some of this design parameter such as stator diameter and stator tooth length will be further adjusted and discussed in Chapter 6 of design optimisation in order to find the best design configuration of the ceiling fan system.

4.4 Conclusion

This chapter explained the stage of constructing the proposed design of the ceiling fan. Some design consideration such as reducing the cogging torque, manufacturing feasibility, high force capability and induced back EMF supported with the literature review discussed in Chapter 2 is conducted in order to produced a good ceiling fan system which capable in generating electricity. The operational idea of the design is further elaborated and the process proceeded with the drawing creation of the model using AutoCAD software which will be used for the simulation stage of the design in the next chapter. Two designs of A and B are created with the different of the presence of reluctant hole in design B.

CHAPTER 5

RESULT AND DISCUSSION

5.0 Introduction

This chapter will explain the simulation stage of the designs proposed in Chapter 4. Our focus is to obtain and study the flux distribution as well as the back EMF of the electrical machine of the ceiling fan. The focus will first be emphasised on the Design A where actual configuration and dimension is used to simulate the real condition of the machine. The simulation are divided into several sub-phases where both part of motor and generator will be detached and simulated separately before it is simulated in one piece.

5.1 Simulation Design

Figure 5.1 shows the Ansoft drawing of the ceiling fan machine proposed in this case study. The model was imported from the AutoCAD model which was designed earlier. In this study, 2D transient analysis is used for the machine which involves the rotation of the magnet rotor. The material for each of the machine components such as stator, permanent magnet, coil and aluminium sheet were pre-defined according to the configuration of the proposed design in Figure 4.2.

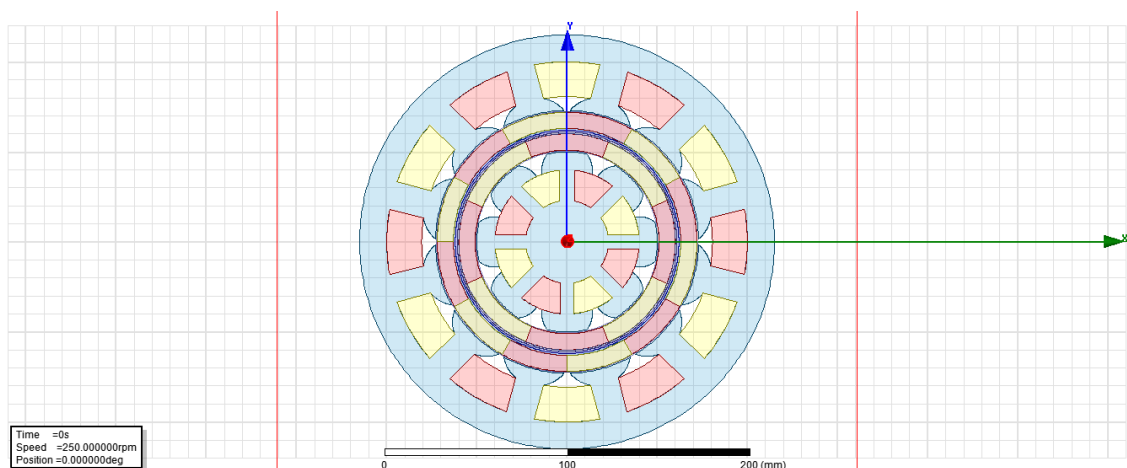


Figure 5.1: Modelled electrical machine

Figure 5.2 and 5.3 shows the separated parts of the electrical machine model of motor and generator parts. The analysis on the flux distribution and back EMF of both parts are conducted separately before both of them are combined in the later part of this section. The motives behind the separation of the motor and generator analysis are for the ease of the model simulation process as well as to ease the tracking of error that might occur during the analysis. With separate part analysis, adjustment of the model configuration can be performed without affecting the other parts of the machine.

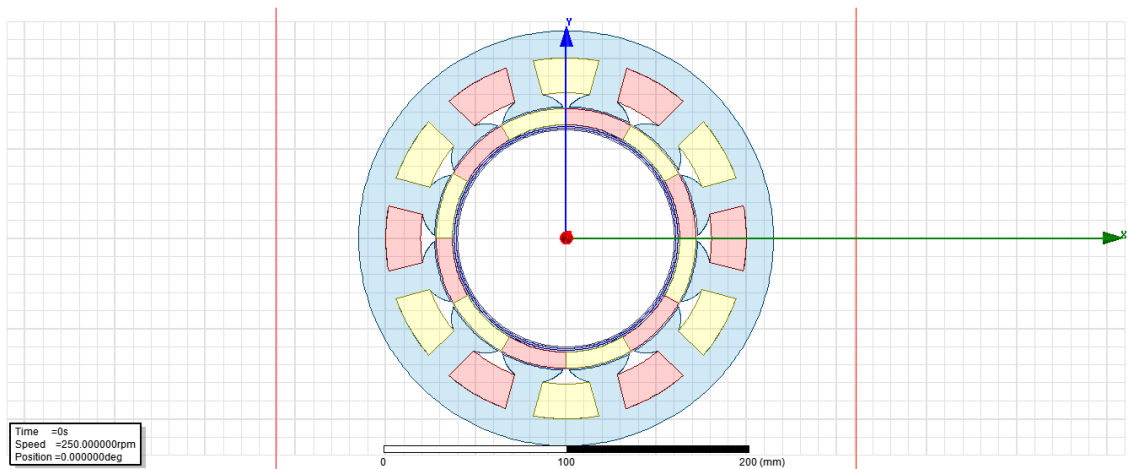


Figure 5.2: Modelled motor part

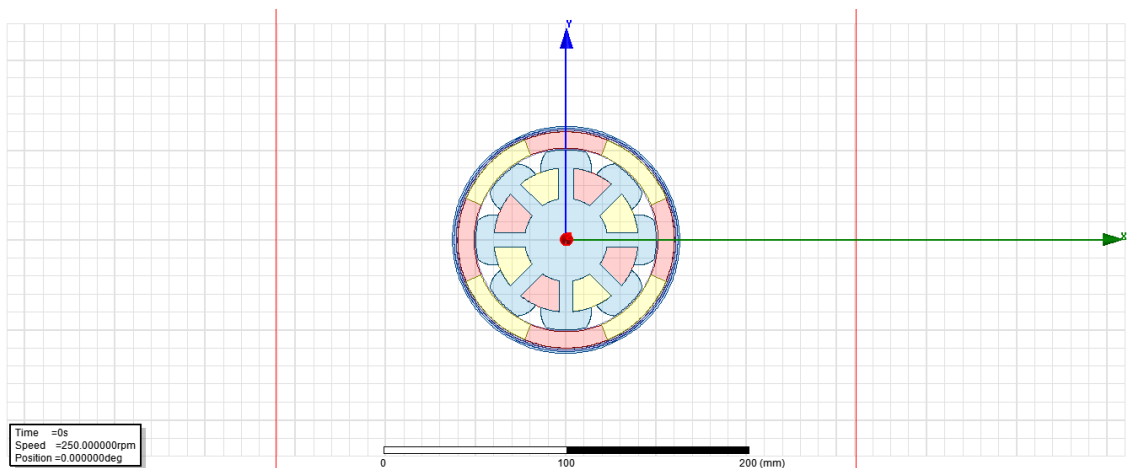


Figure 5.3: Modelled generator part

5.2 Meshing Operation

The modelled drawings of both machine parts are meshed as the next step of the analysis process. Meshing process is a part of computer-aided engineering (CAE) where the geometry of the selected model will be discretised automatically into small triangles in order to solve the set of algebraic equation [14]. The number of mesh affects the accuracy, speed and convergence of the solution. The higher the number of meshing, the better the solution but more time is consumed for the analysing process.

Figure 5.4 and 5.5 show the meshing of both modelled part drawing as well as the combined electrical machine. The models need to be meshed for the software to perform the analysis process on the designs. For this study, the meshing operation is limited to 1000 maximum elements due to the restricted performance of the computer. Higher mesh element number might cause the computer performance to be slow and delay the analysis process for the modelled electrical machine.

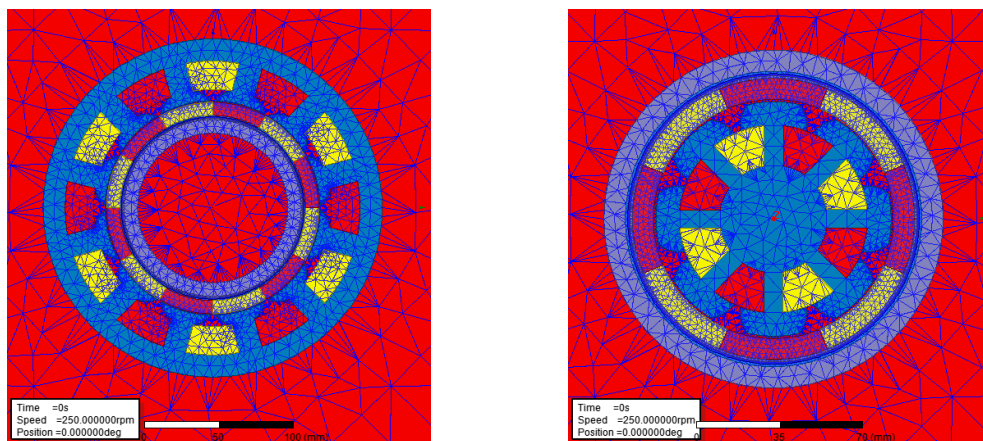


Figure 5.4: Meshed motor part and generator part

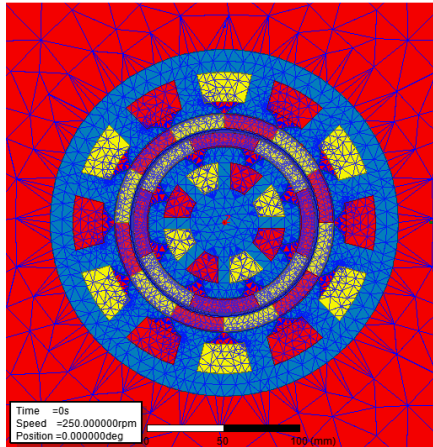


Figure 5.5: Meshed combined electrical machine

5.3 Simulation Result

5.3.1 Flux Distribution

From the meshed motor and generator part of model, the simulation of the modelled designs was conducted to study the characteristic of flux distribution and the back EMF of the motor and the generator. The vector directions for flux distribution of the rotor permanent magnet need to be right before we can proceed with advance rotary analysis of the models. In order to make sure the flux distribution for the permanent magnet is correct, the model is being simulated in static condition (0 rpm) with 0A current from the coil. The result of the static flux distribution for the design model is shown in Figure 5.6 and Figure 5.7 below.

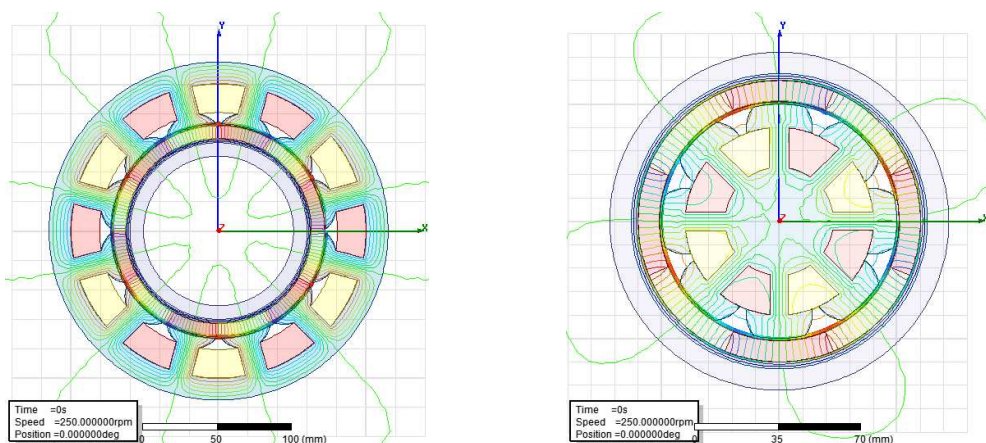


Figure 5.6: Open flux distribution of motor and generator part

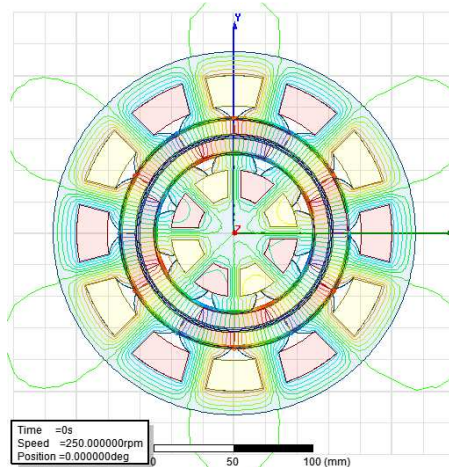


Figure 5.7: Open flux distribution of electrical machine

The flux distribution characteristic for the design is correctly proved where the flux is going out from the North-oriented permanent magnet (red) and flowing into the South-oriented permanent magnet (yellow). Since the North-pole and South-pole of the magnet is placed side by side with the same magnetic field, the magnetic flux from the N-pole will be evenly distributed where half of the flux will go into the left side S-pole while the other half go into the right side S-pole in open air. With the presence of laminated iron core stator, the flux will be directed to flow into the stator and return back to the nearest S-pole magnet.

After confirming the right flux distribution of the permanent magnet rotor, the rotating analysis of the electrical machine is carried out. Motion band for the model is assigned in the software where the rotor part of the model will be rotate according to the input parameter of the motion band. The rotor part of the ceiling fan machine is set to be rotate at a constant speed of 250rpm (15° rotation every 0.01s) and the flux distribution will be studied and observed.

Figure 5.8, 5.9 and 5.10 show the transient flux distribution of the rotated permanent magnet rotor with respect to the rotation angles. The flux distribution of the design models were being traced at every 45° of rotor rotation. From the result, the flux distribution for each angle is different and was reported to keep changed due to the change in the position of the permanent magnet rotor. The flux behaviour for each rotating angle follows the expected flux characteristic that had been discussed earlier.

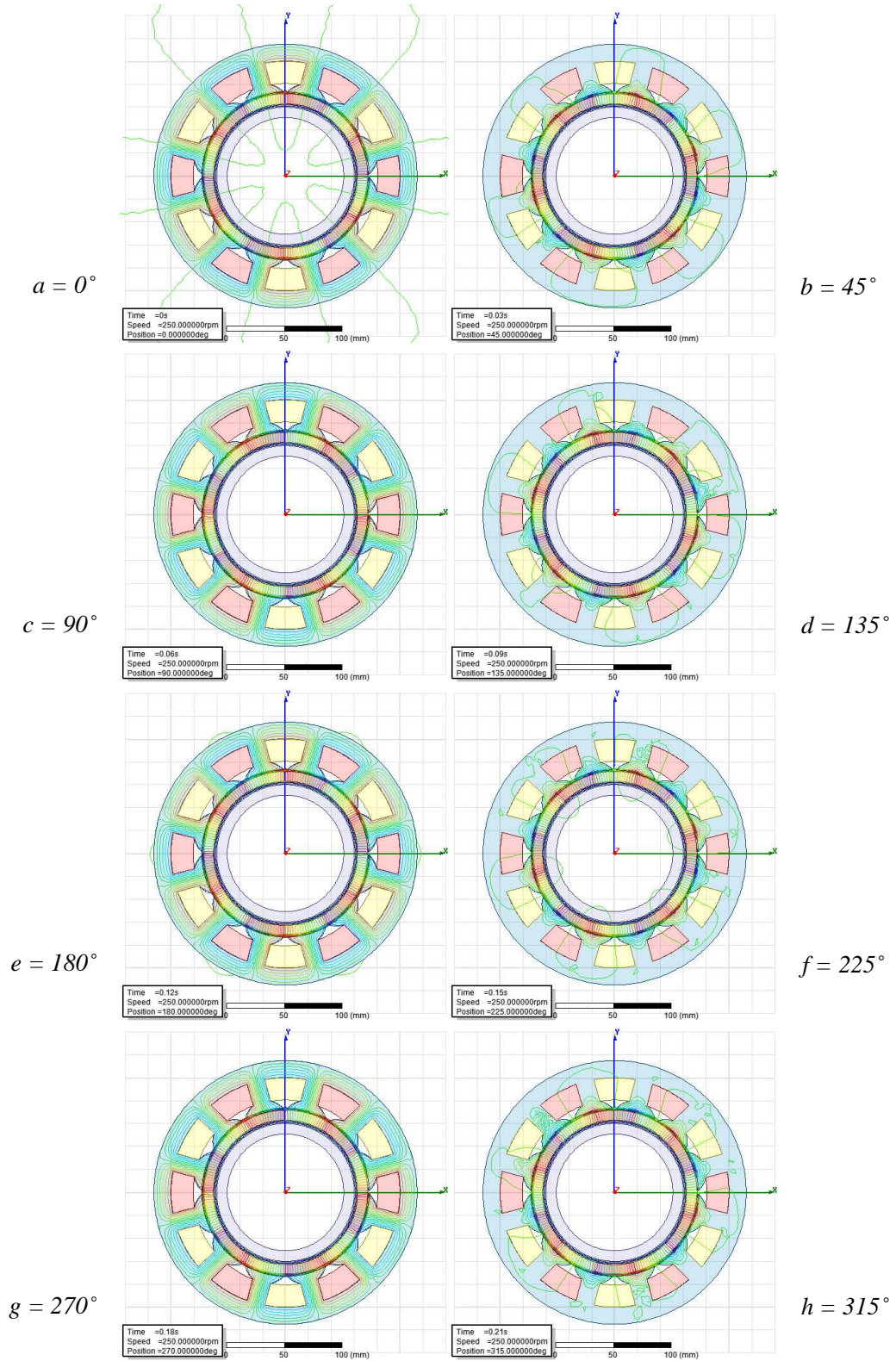


Figure 5.8: Transient flux distribution of motor part

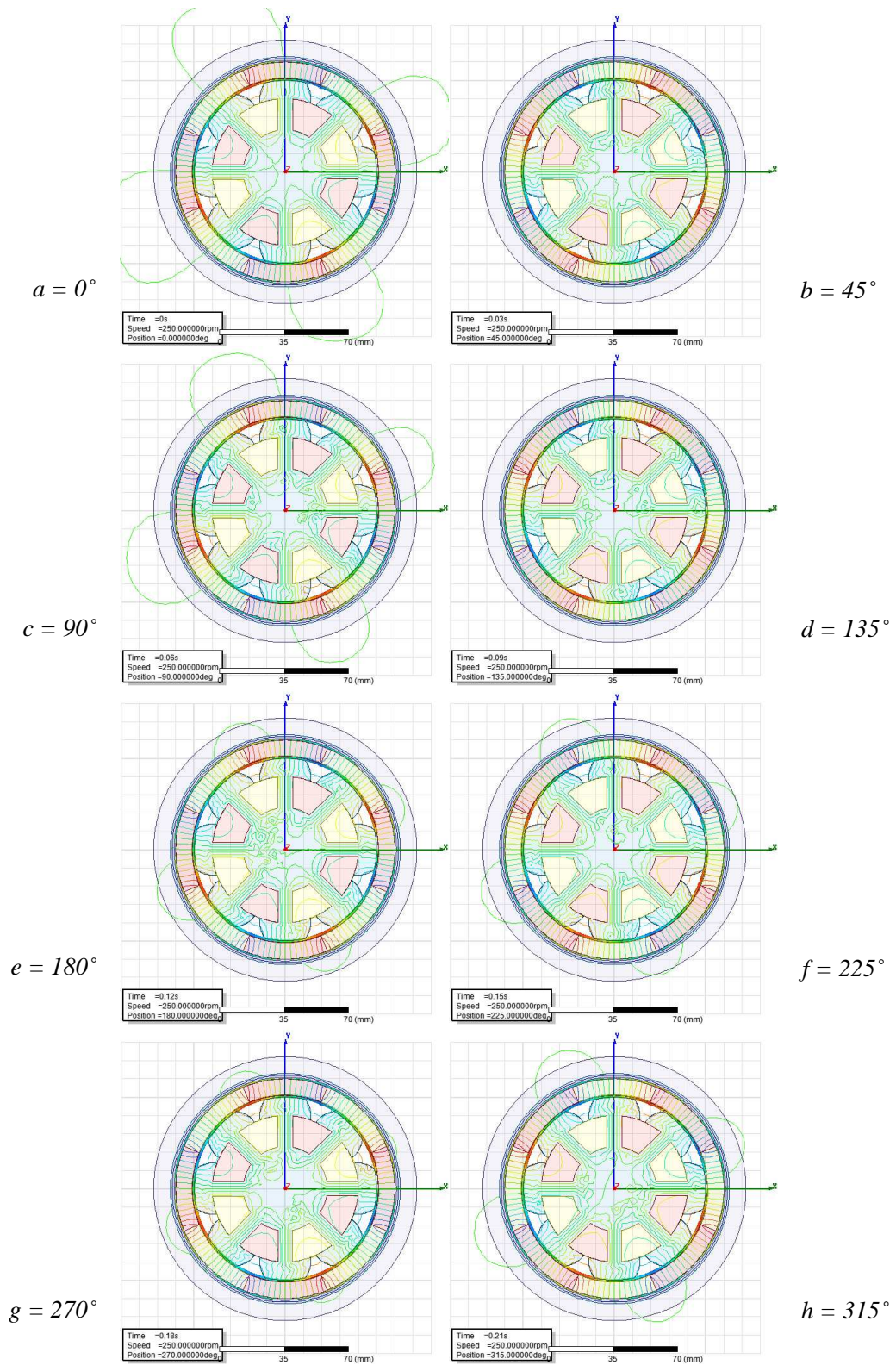


Figure 5.9: Transient flux distribution of generator part

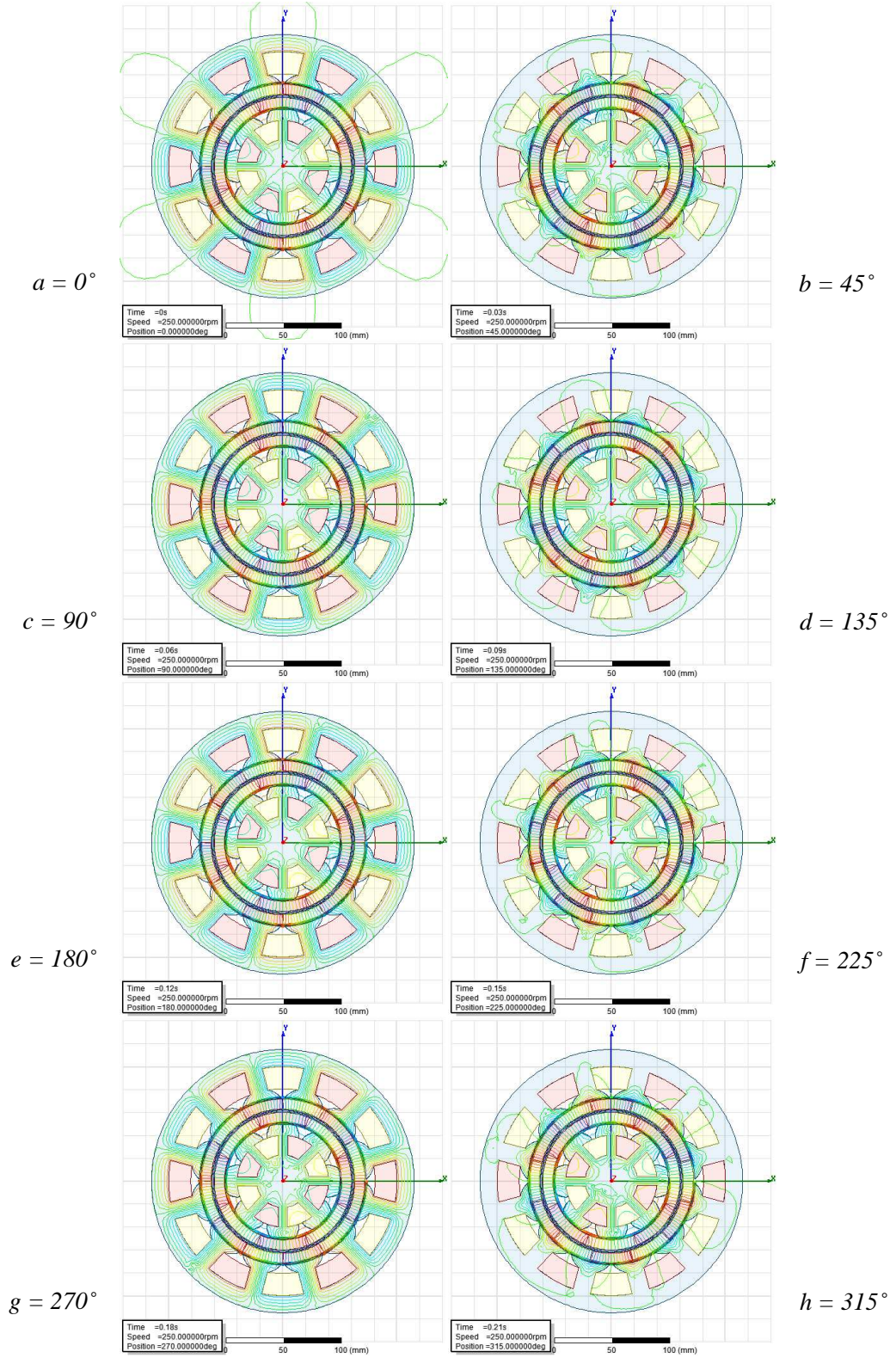


Figure 5.10: Transient flux distribution of combined electrical machine

5.3.2 Air Gap Flux Density

Based on the flux distribution obtained from the simulation, the plot of air gap flux density of both motor and generator can be obtained by using the same finite element software. Flux density is defined as how intense the flux lines are in a given unit area. This intensity is shown by the closeness of the flux lines in the diagram. The more intense the flux lines, the higher the flux density it will produce. The flux density is usually higher as it moves closer to the magnet pole.

To measure the flux density of the air gap between the motor and stator of model, two arc lines were drawn on both air gaps of motor and generator. The arc lines were drawn circulating the air gap circumference perimeter and were positioned so that they lie right in the centre of the air gap to get the average measurement of the air gap flux density. Figure 5.11 shows the positioning of the arc line in determining the trend of flux density of the air gap for both motor and generator parts.

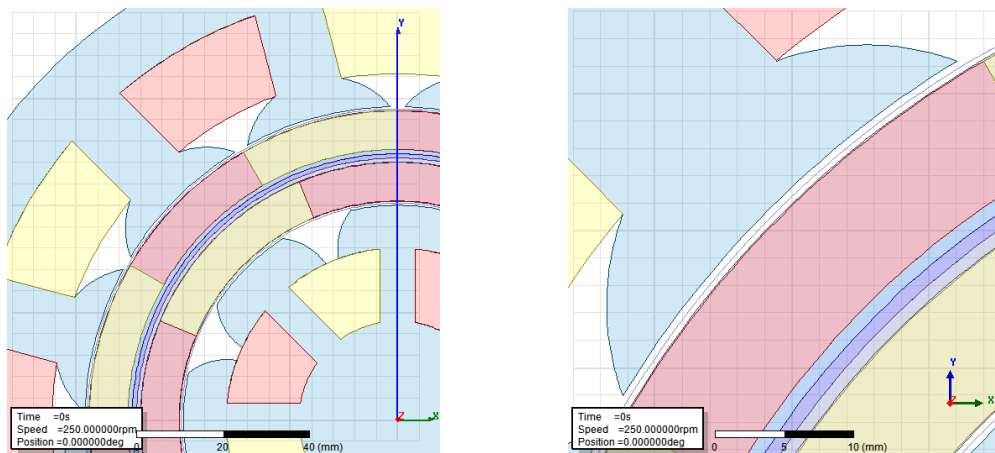


Figure 5.11: Arc line positioning in determining air gap flux density

Figure 5.12 and 5.13 plot the distribution of flux density along the air gap of the motor and generator respectively. The winding coil is set to be 0A to avoid any interference resulted from the induced flux of the current-carrying winding coil. The graph plots were being traced at the initial position of 0° where the rotor is about to rotate. During this position, each of the stator teeth is completely facing the magnet pole of the rotor where the flows of flux into the stator tooth are at its maximum.

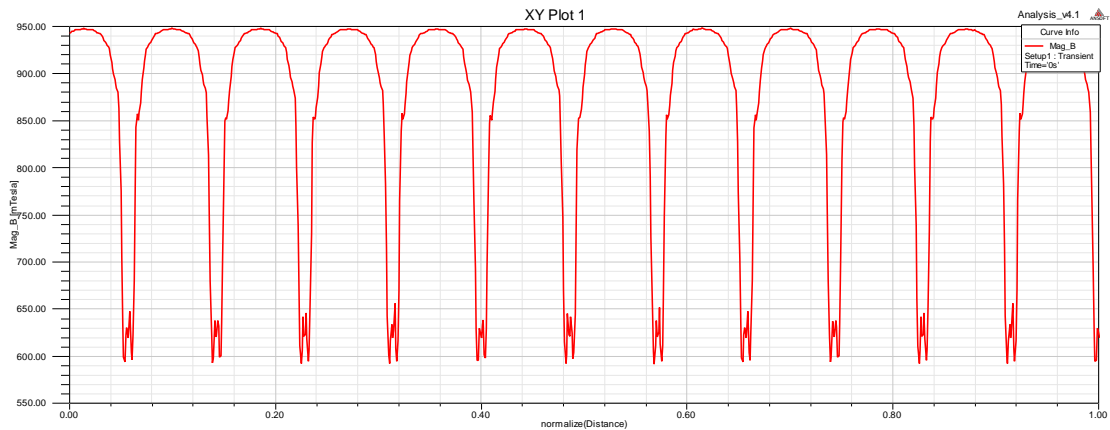


Figure 5.12: Air gap flux density of motor part

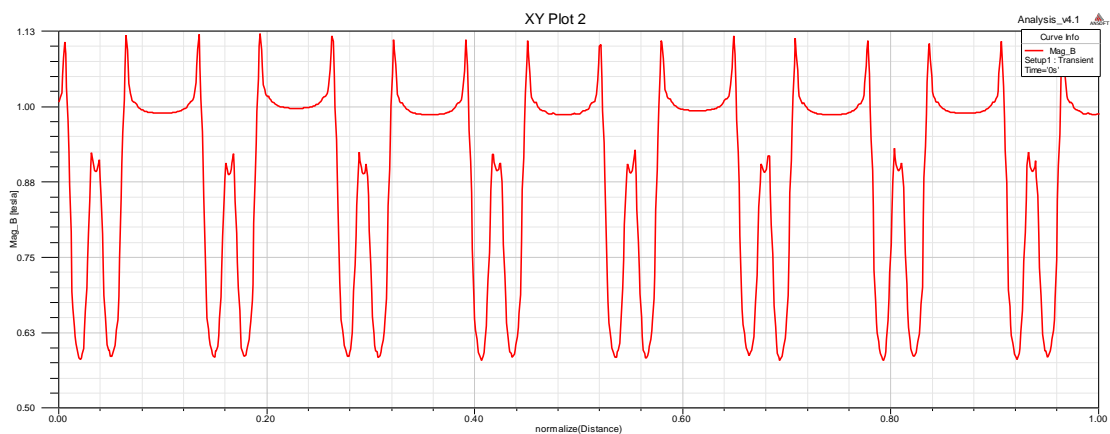


Figure 5.13: Air gap flux density of generator part

Based on the observation trend of air gap flux density of both parts, each of the sine wave graphs represents the flow of flux into the stator tooth. The flux density increases as it approaches the stator tooth as the magnetic flux tends to flow into a medium such as iron which has good magnetic conductor properties as compared to air. The drop in flux density which is shown on both graphs indicates the region in between the stator tooth where the distribution of the magnetic flux line is the least.

From the graphs, the magnetic flux density produced at the motor stator side is approximately 0.95 Tesla. Meanwhile, an approximate of 0.97 Tesla of magnetic flux density is produced at the generator stator side. With the flow of magnetic flux into the stator, we can confirm that there is possibility in generating electricity at the inner stator which represents the generator.

5.3.3 Back EMF

As the speed of the motor increases the resulting back EMF also increase. To obtain the back EMF of the proposed ceiling fan model, winding coils need to be introduced on the simulation. In this case study, the number of winding copper wire for each of the teeth is set to be 250 turns of coil. The arrangement of the winding coil is made so that the direction of the coil-turns is alternating for each tooth thus allowing one direction of current flow for each slot. The current for both winding is set to be 0A.

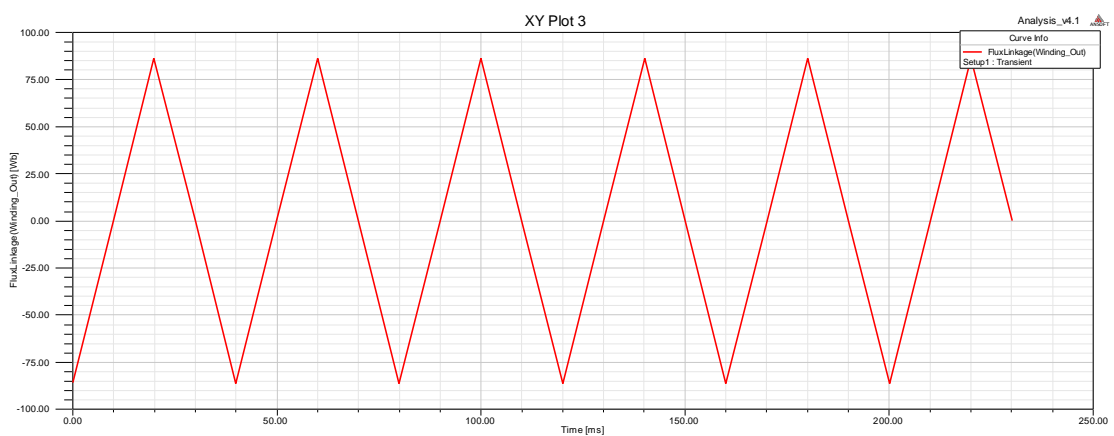


Figure 5.14: Flux linkage of motor winding

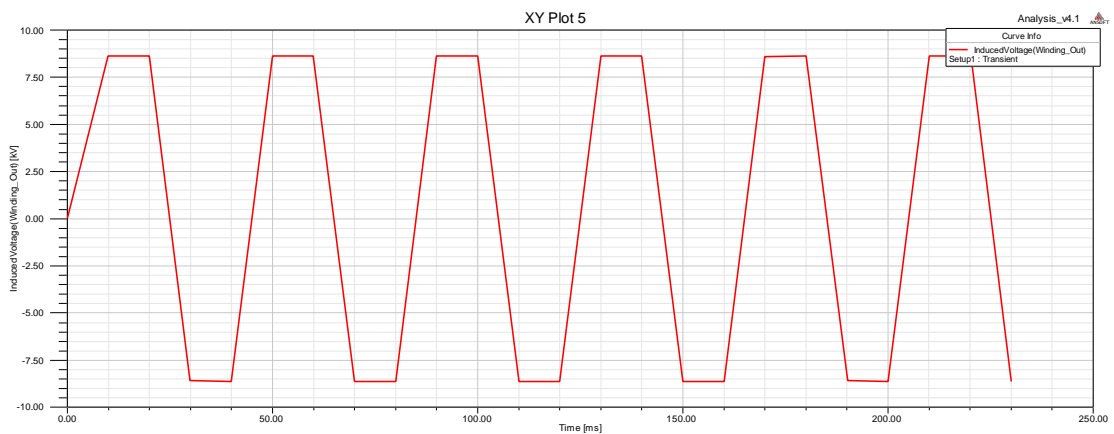


Figure 5.15: Induced voltage of motor winding

Figure 5.14 and 5.15 show the flux linkage as well as the induced voltage of the outer winding (motor part) resulted from the simulation. Flux linkage is defined as the amount of magnetic flux threading the coil, multiplied by the number of coil turns. The flux linkage across the coils is affected by the number of coils turn as well as the strength of

the magnetic field. It is observed that the voltage induced from the stator winding is proportional with the flux linkage as the result of the rotor rotation which satisfies the following equations;

$$\lambda = \int v dt$$

$$v = \frac{d\lambda}{dt}$$

$$\lambda = \int_S \vec{B} \cdot d\vec{S}$$

where λ is the flux linkage in Weber, v is the induced voltage and B is the flux density vector per unit area.

From the graph plotted in Figure 5.15, the induced voltage of the motor part is in ac voltage with the rms value of 8.43 kV. Note that the simulation was being conducted in 2D transient analysis with the default setting of 1 meter height for the model design. Therefore, the actual amount of the induced voltage for the motor part assuming the design is 7mm in height can be calculated as follows:

$$voltage_{rms} = \frac{voltage_{rms,1m}}{1000} \times height(mm)$$

$$voltage_{rms} = \frac{8.43kV}{1000} \times 7 = 59.01 V$$

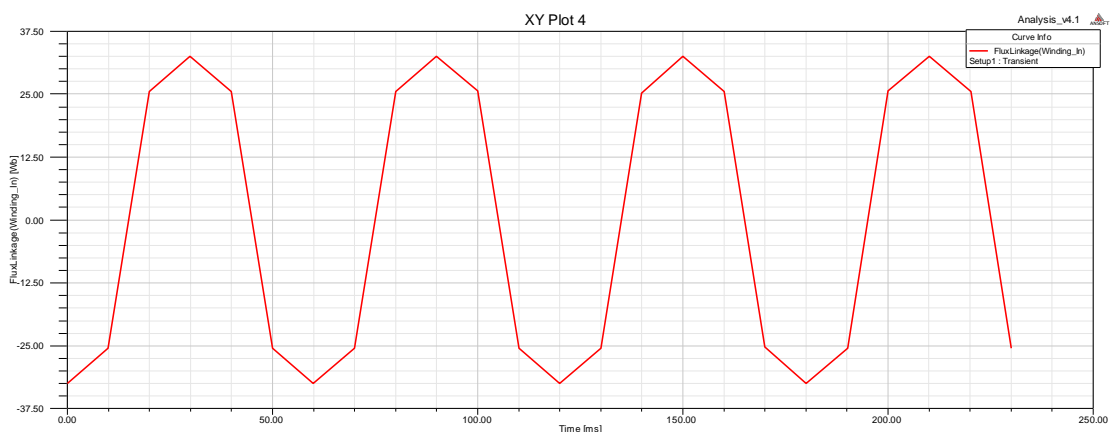


Figure 5.16: Flux linkage of generator winding

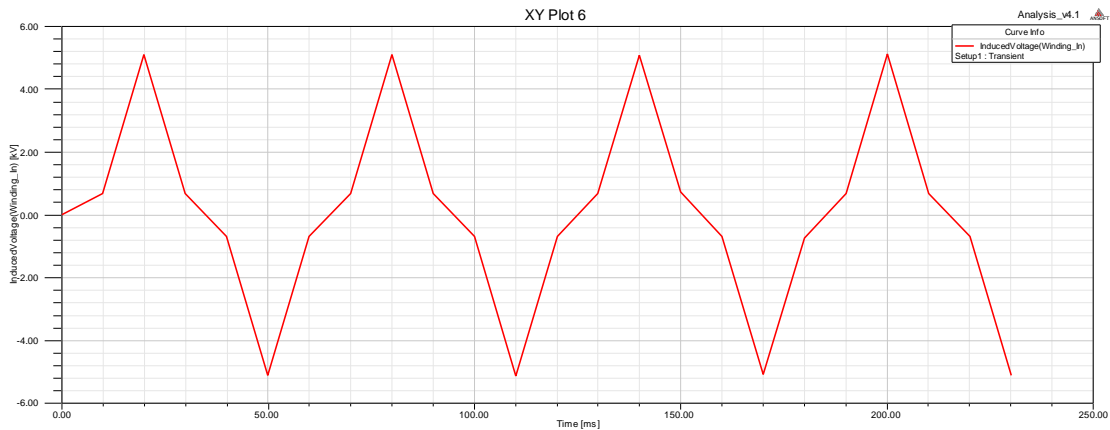


Figure 5.17: Induced voltage of generator winding

Meanwhile, Figure 5.16 and 5.17 show the flux linkage and the induced voltage of the inner winding (generator part) of the model. Based from the graph, similar with the motor part, the induced voltage is proportional with the flux linkage produced. The amount of the induced voltage for the generator part based on the plot shows in Figure 5.17 is 2.99 kV rms value. Assuming the actual height of the ceiling fan machine to be 7mm, the induced voltage for the generator part is calculated as follows:

$$voltage_{rms} = \frac{2.99kV}{1000} \times 7 = 20.93 V$$

The generated voltage for both parts are based on the open circuit voltage drop without any flow of current, the generator need to be connected to the load in order to calculated the power produced by the generator part of the proposed design. Assuming the generator is connected to a bulb with resistive value of 240 Ω , the generated power is calculated as the following:

$$P = \frac{v^2}{R}$$

$$P = \frac{20.93^2}{240} = 1.8W$$

5.4 Performance Analysis

After completing the simulation and performance analysis for Design A in term of the flux distribution, air gap flux density as well as the back EMF of the model, the study will be proceed with the simulation of Design B which have the additional features of reluctant hole inside the stator tooth of both motor and generator part. The simulation result of Design B will then be compared with the previous Design A to find the best configuration of the electrical machine ceiling fan.

The simulation procedure for the design B is kept to be constant for the ease of comparison and analysis in term of the model performance between the two proposed designs. Reluctant holes or notch features will be added into the stator using the same software of AutoCAD. As the design B been uploaded into the Ansoft Maxwell software, the notch area will be set to vacuum, to imply the reluctant holes are the gap passing through the stator tooth.

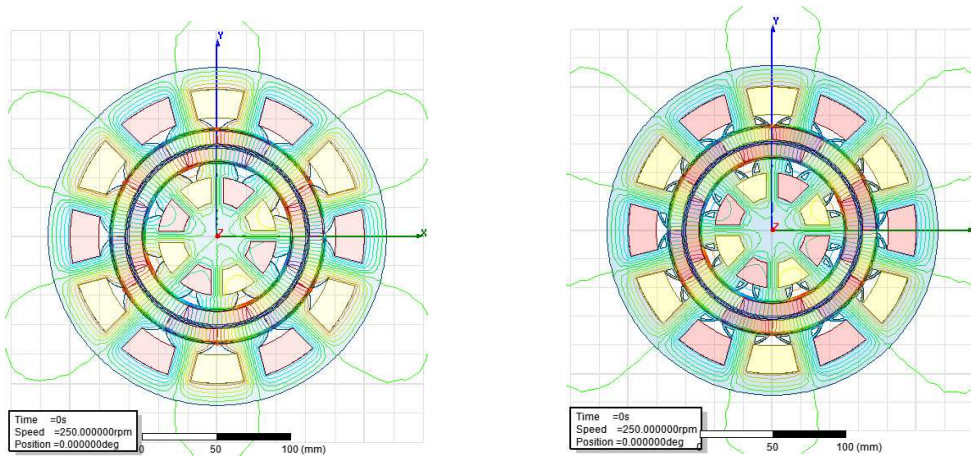


Figure 5.18: Flux distribution of design A and B

Figure 5.18 shows the flux distribution comparison between design A and B. The flux distribution for both designs are proven to be correct where the magnetic flux had been observed to accurately flow out from the North-pole magnet and returned back into the South-pole magnet through the iron stator. Reluctant holes according to the study done by Gizaw D. [12] might be helpful in reducing the cogging torque and allows a smooth surface of the pole and improves the motor demagnetisation margin.

Figure 5.19 and 5.20 show the comparison in the air gap flux density of design A and B which denotes by red and blue colour respectively.

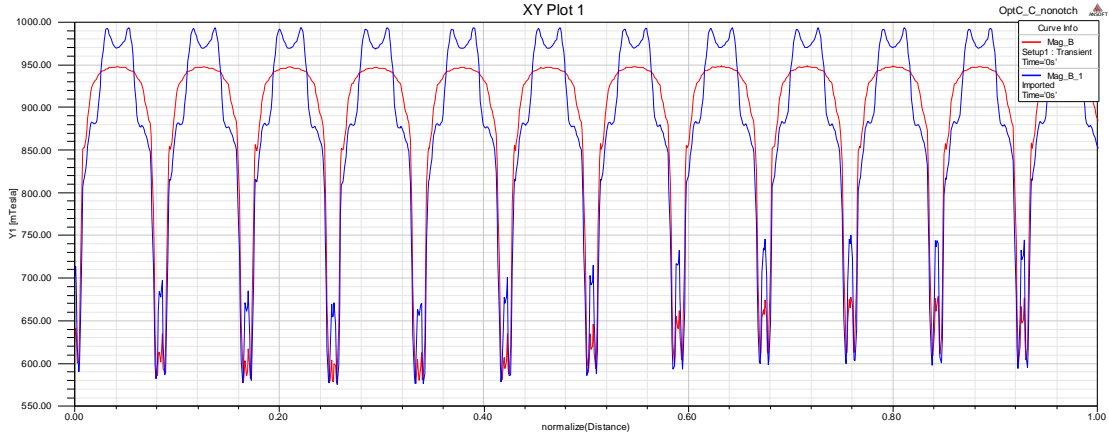


Figure 5.19: Air gap flux density of design A and B (motor part)

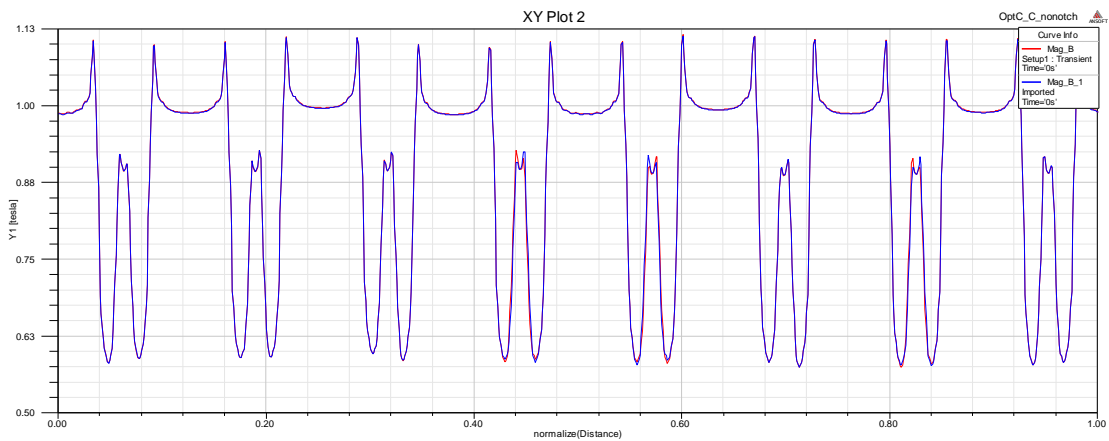


Figure 5.20: Air gap flux density of design A and B (generator part)

From the observation of performance plot in Figure 5.19, the flux density had been observed to be higher for the design B (blue plot) however with the narrower tip as compared to design A (red plot). With the presence of reluctant holes in design B, the flux collected by the tooth tip of the stator, due to the narrow tooth tip caused by the presence of the notch, will be directed to the centre of stator tooth thus resulting in compressing the flux line in the middle area of the tooth. This explains the reason behind the higher and narrower flux density as compared to design A.

The air gap flux density for the generator part as shown in Figure 5.20 however shows insignificant difference in the flux density possibly due to the smaller reluctant holes.

Figure 5.21 and 5.22 shows the comparison in the induced voltage of design A and B represented by red and blue colours respectively.

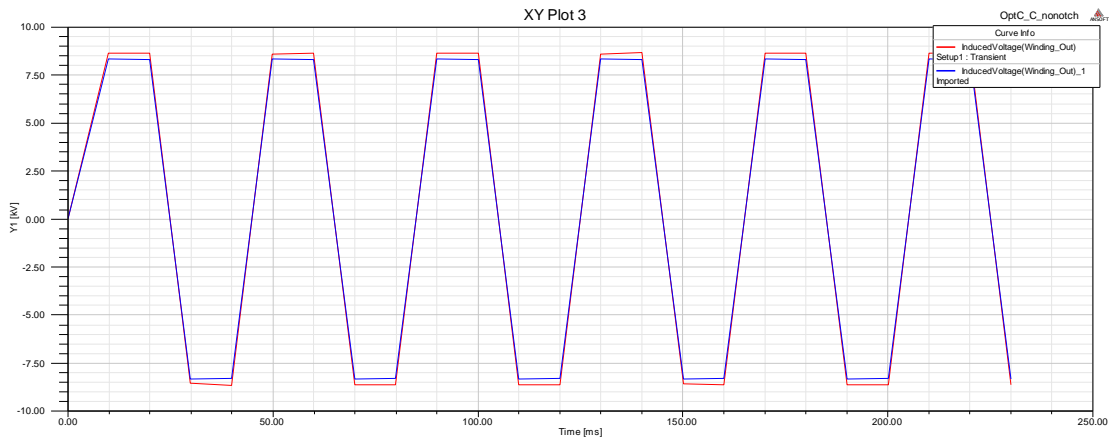


Figure 5.21: Induced voltage of design A and B (motor part)

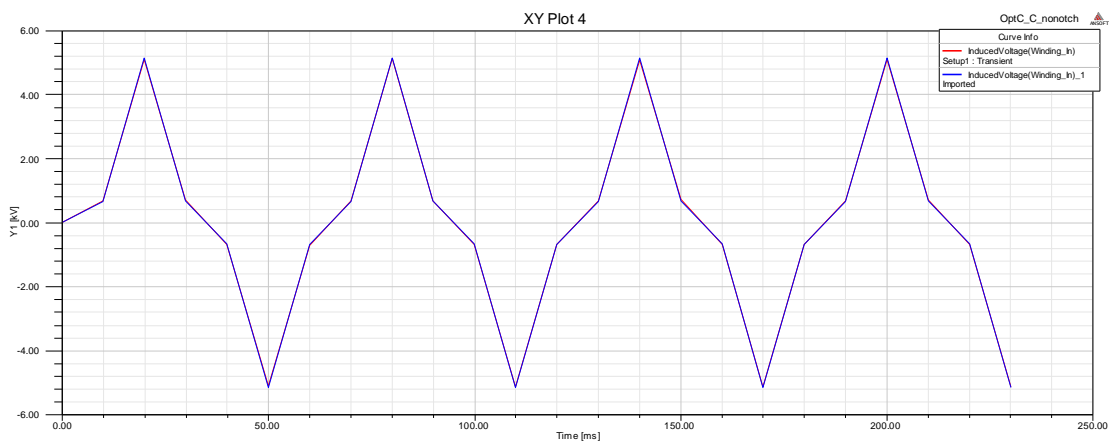


Figure 5.22: Induced voltage of design A and B (generator part)

Design	A (no notch)	B (with notch)
Induced voltage, V (motor part)	59.01	56.91
Induced voltage, V (generator part)	20.93	19.81

Based on the performance plot shown in Figure 5.21 and 5.22, design A is observed to produce higher induced voltage for both motor part and generator part as compared to design B. Although the reluctant holes are expected to reduce the cogging torque of the ceiling fan machine, the back EMF produced by design B however is lower as compared to design A. Therefore, design A is selected as the best configuration and will be used for the next design optimisation.

5.5 Conclusion

This chapter explained the simulation stage of the proposed designs by using the finite element software of Ansoft Maxwell. The drawing designs were imported from the AutoCAD into the software for the simulation. The component material and magnetic characteristic of the permanent magnet rotor is defined before the simulation process. The results obtained are focused on the flux distribution, air gap flux density and the back EMF of both models. Both designs A and B showed a good characteristic of the flux distribution and the air gap flux distribution and both designs are proved to be capable in generating the electricity. Based from the performance comparison of both design, design A which produce a higher induced voltage compared with B is selected. The selected design A will be further modified for the optimisation stage which will be discussed in the next chapter.

CHAPTER 6

DESIGN OPTIMISATION

6.0 Introduction

From the obtained simulation results of the model designs discussed in Chapter 5, the studies is now advanced into the next phase as to comply the fourth objective of the case study which is design optimisation. The purpose of the optimisation is solely to improve the model performance in term of the induced voltage. Some of the design parameter is adjusted while maintaining the other parameter to observe the performance feedback of the ceiling fan. Two design optimisation will be conducted in this chapter which is split ratio variation and pole pitch ratio variation.

6.1 Variation of Split Ratio

6.1.1 Optimisation Design

One of the adjustments made for the optimisation of the design is the variation of the design split ratio. Split ratio in this case study is defined as the ratio of the generator diameter, d_i over motor diameter, d_o which is illustrated in Figure 6.1. The generator diameter of d_i is measured from the one end of the inner magnet rotor of the ceiling fan to the other end of the magnet, passing through the origin point. The fixed diameter of the motor, d_o is measured from the design outermost diameter.

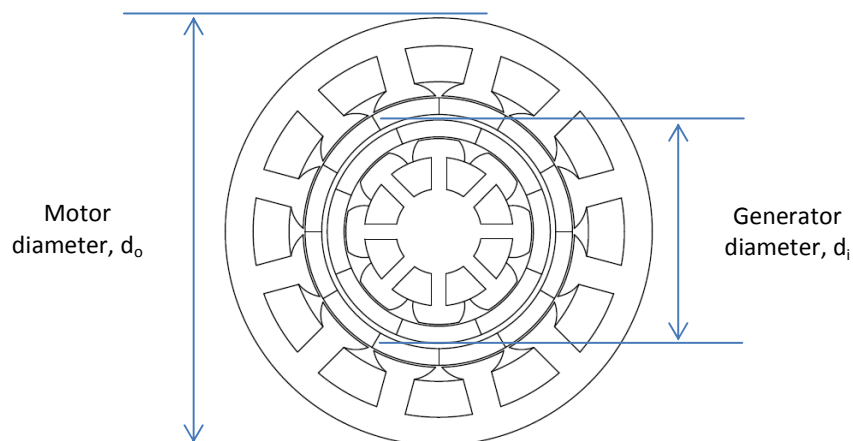
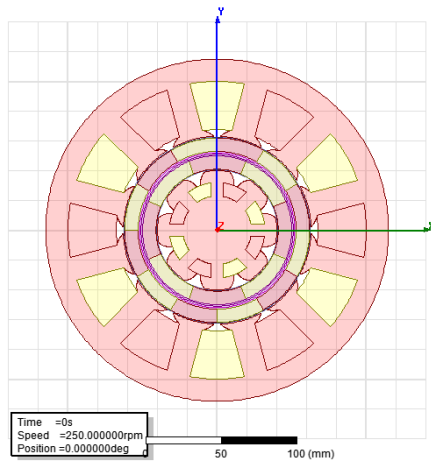
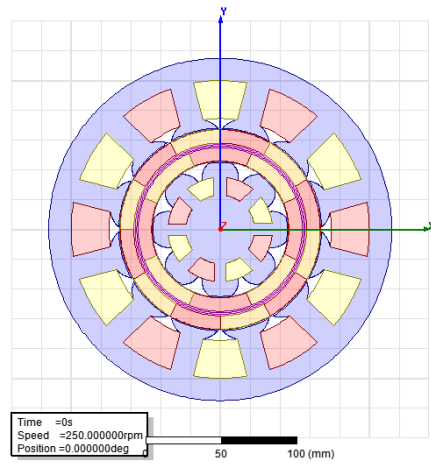


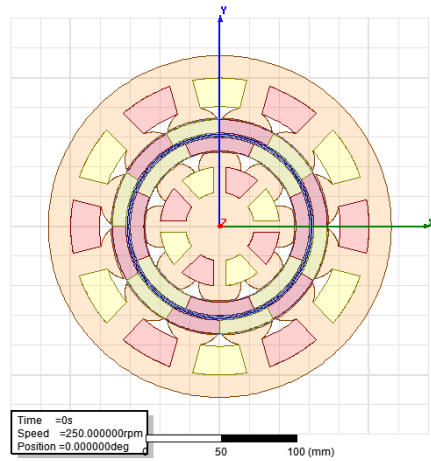
Figure 6.1: Design split ratio



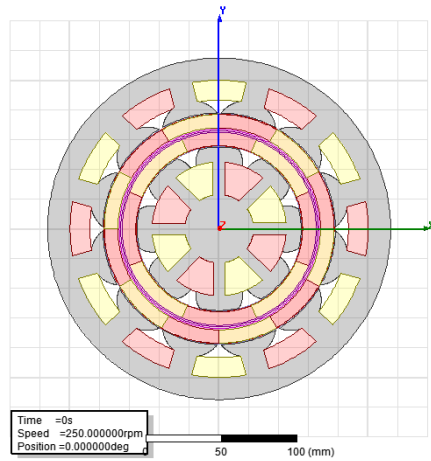
Variation S1
Split ratio: 0.43



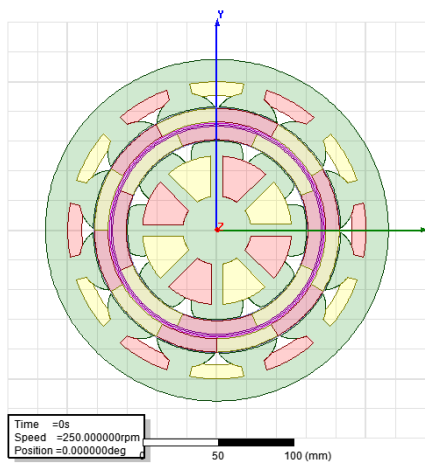
Variation S2
Split ratio: 0.48



Variation S3 (default)
Split ratio: 0.52



Variation S4
Split ratio: 0.56



Variation S5
Split ratio: 0.60

Figure 6.2: Designs with split ratio variation

The default design of the ceiling fan has a split ratio of 0.52. In order to further optimise the current design of the ceiling fan model, four additional variations of design were created using AutoCAD by adjusting the generator diameter without changing other design parameter with the increment/decrement of 10mm diameter between each design. Figure 6.2 shows five variation design of the ceiling fan model with different split ratio as referred to Table 6.1. Each of the variation is then simulated using the Ansoft Maxwell software to obtain the result. The focus will be emphasised on the induced voltage of the model design.

Table 6.1: Variation of split ratio

Variation	S1	S2	S3	S4	S5
Split ratio	0.43	0.48	0.52	0.56	0.60
Generator diameter, d_i (mm)	100	110	120	130	140
Motor diameter, d_o (mm)	230	230	230 <td 230	230	

6.1.2 Optimisation Result

The simulation setting and procedure for all five variations is kept to be constant to avoid the possibility of repeatability error as well as to observe the result performance more precisely. From the simulation results obtained, the plot for each variation will be layered together to aid the performance observation and comparison. Figure 6.3 and 6.4 show the air gap flux density for both motor and generator of the variation S1, S2, S3, S4 and S5.

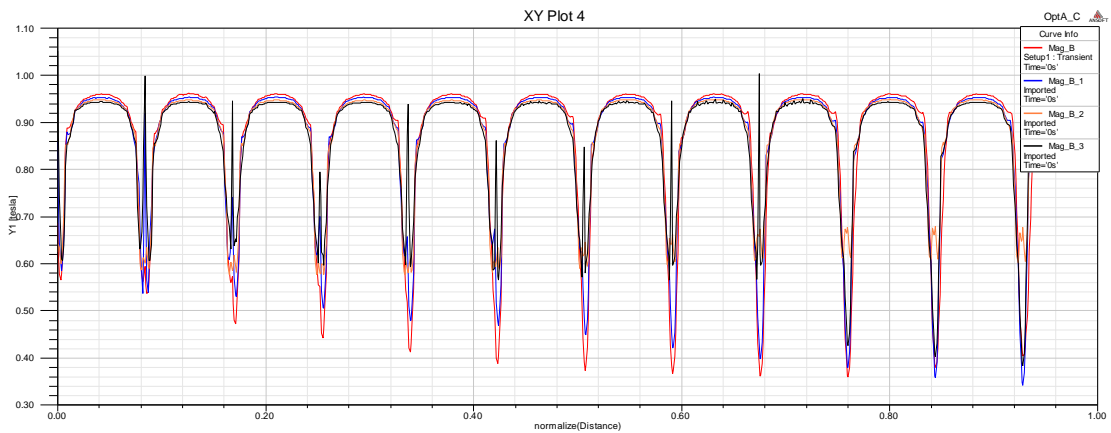


Figure 6.3: Air gap flux density of variation S1, S2, S3, S4 and S5 (motor part)

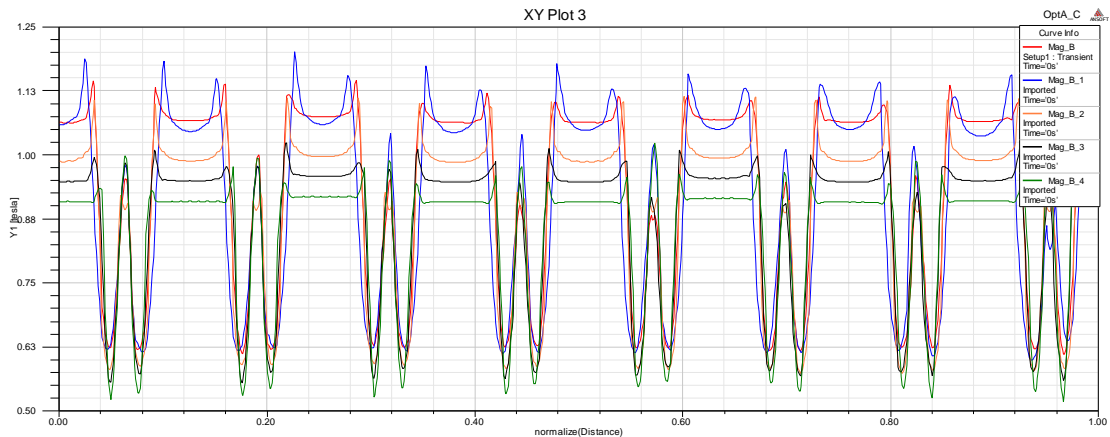


Figure 6.4: Air gap flux density of variation S1, S2, S3, S4 and S5 (generator part)

Similar to the previous section, the winding coil is maintained at 0A to avoid any flux interference resulted from current-carrying coil. Both graph plots were being traced at the air gap line between the rotor and stator at the initial position of 0° where the flux flows from the magnet rotor into the stator tooth are at its maximum. Each graph contains five plots of air gap flux density denotes by the colour of red, blue, orange, black and green which represent variation S1, S2, S3, S4 and S5 respectively.

Based from the Figure 6.3, variation S1 shows the highest magnetic flux density at the air gap region of motor part which is approximately 0.96 Tesla, followed by variation S2, S3, S4 and S5 in descending order. Same trend occurred for the air gap flux density of the generator part as shown in Figure 6.4 where variation S1 produces the highest flux density amount of approximately 1.5 Tesla with similar descending manner.

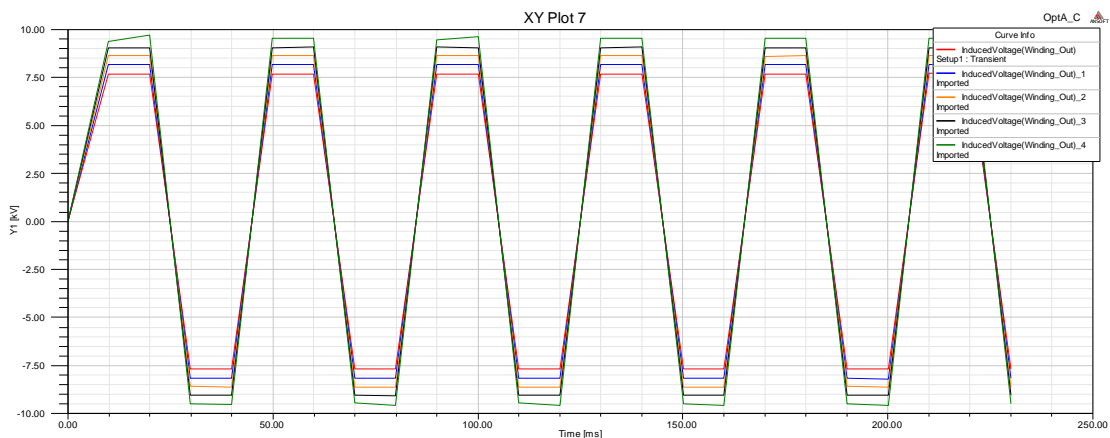


Figure 6.5: Induced voltage of variation S1, S2, S3, S4 and S5 (motor part)

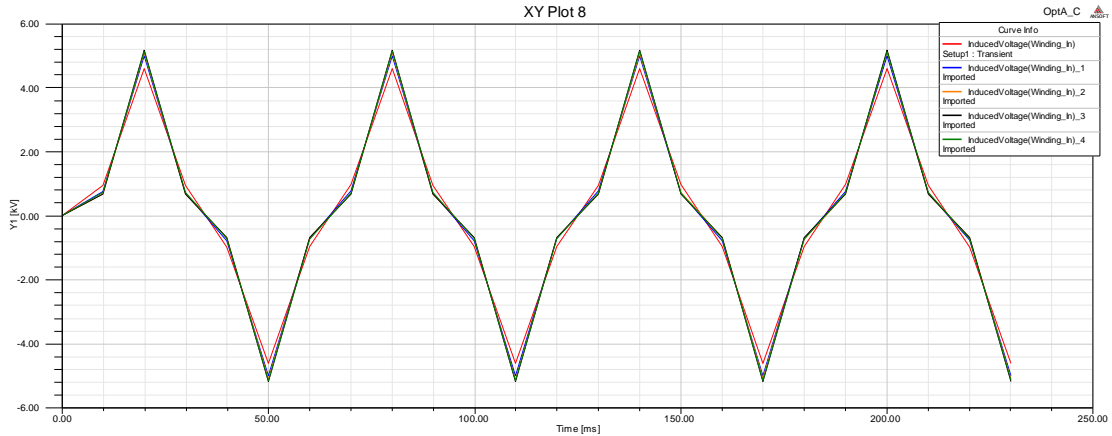


Figure 6.6: Induced voltage of variation S1, S2, S3, S4 and S5 (generator part)

Figure 6.5 and 6.6 shows the plots of the induced voltage of different split ratio variation for motor and generator respectively. Based on the rough observation on the graph, all the designs produce a similar trend of induced voltage plot however with different magnitude. The rms value of induced voltage for each variation is tabulated and then plotted as shown in Table 6.2 and Figure 6.7.

Table 6.2: RMS value of induced voltage (split ratio)

Variation	S1	S2	S3	S4	S5
Split ratio	0.43	0.48	0.52	0.56	0.60
Induced voltage (outer winding). V	52.64	55.93	59.01	61.88	65.17
Induced voltage (inner winding). V	19.39	20.58	20.93	21.21	21.14

From the performance plot in Figure 6.7, two dissimilar trends of performance plot were identified between the motor and the generator part as the split ratio of the design varies. For the motor part, variation S5 with the split ratio of 0.60 is observed to yield the highest induced voltage of 65.17 V followed by S4, S3, S2 and S1 in the descending manner. For the motor part, the induced voltage had been observed to increase as the split ratio increases. In another word, the voltage induced by the motor stator rises with the increment of the magnet length.

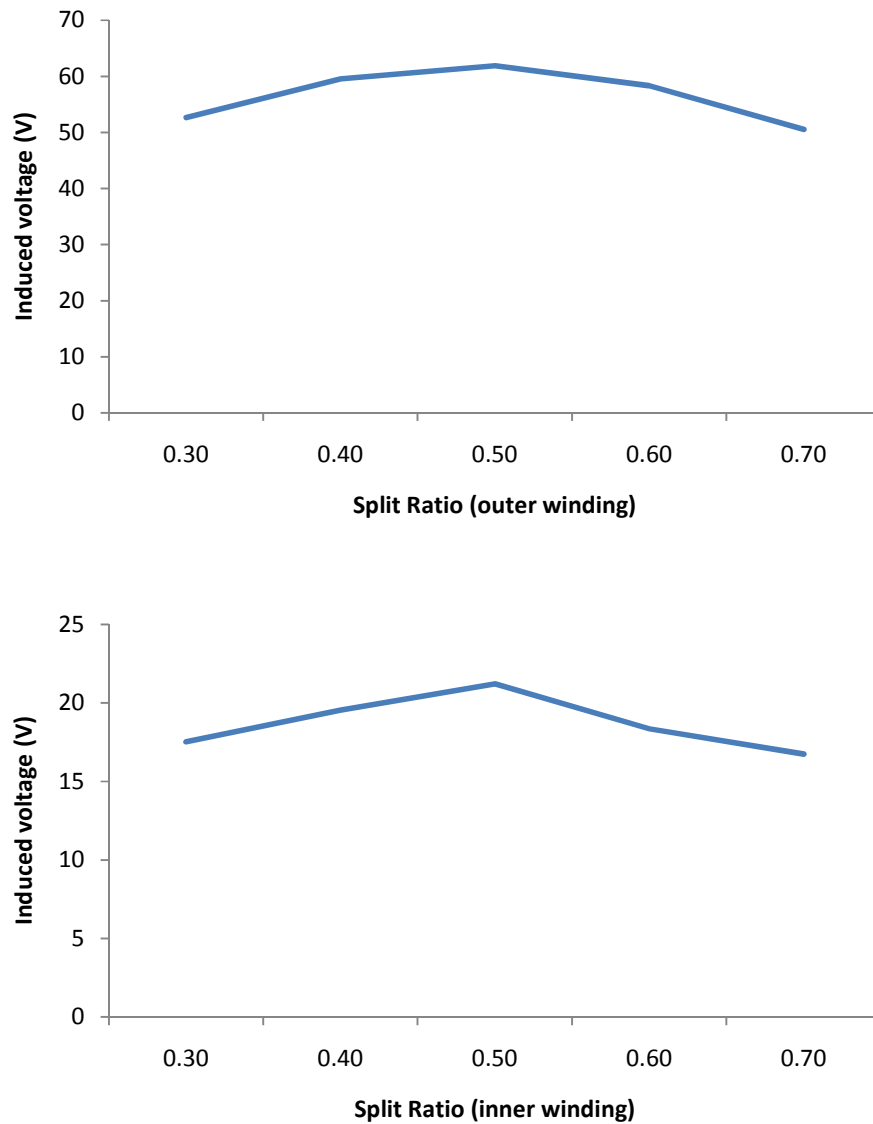


Figure 6.7: Performance plot of split ratio optimisation

This is possibly because as the split ratio increase, the perimeter of the magnet rotor increases proportionally. Increasing in the magnet size will increase the flux density produced by the magnet rotor, therefore the back EMF produced will also increases proportionally. Higher magnetic flux density will flow into the stator thus resulted in higher voltage being induced by the winding coil.

However, generator part of the machine design shows a different trend of performance plot in term of the induced voltage as compared to the motor part. The graph plot is first

observed to increase as the split ratio increase implying the magnetic flux increase with the magnet rotor size until the turning point ratio of 0.56 where the voltage induced by the generator had been observed to start decreasing afterwards. The induced voltage for the generator part is decreasing despite the increment of the magnetic field of the magnet.

The decrement in the induced voltage for split ratio larger than 0.56 is large possibly due to the big slot area of the stator winding created as the result of increasing the diameter of the generator while maintaining the number of winding coil and the thickness of the stator tooth. As the generator diameter increase with the increase in the split ratio, the increasing tooth length and slot area resulted in increasing the area coverage for the winding coil. Therefore, less flux will be captured by the copper coil winding which resulted in less voltage being induced by the generator.

This problem of decreasing induced voltage can be solve by reducing the slot area by doubling the stator slot or increasing the number of stator winding coil. However, the cost in doubling the stator tooth as well as increasing the magnet size for the ceiling fan might be expensive and not suitable for the purpose of mass production. Therefore variation S4 with the split ratio of 0.56 is selected as the optimised design. This design will be used for the next design optimisation replacing the original proposed design.

6.2 Variation of Pole Pitch Ratio

6.2.1 Optimisation Design

Another adjustment made for the design optimisation is the variation of the design pole pitch ratio. Pole pitch ratio in this context is defined as the ratio of the arc length angle of the north-pole magnet, x_n over the arc length angle of the magnet rotor pole pair, x_t which is illustrated in Figure 6.8. The angle of the north-pole magnet is measured based on the tip-to-tip angle of the magnet itself while the fixed angle measurement of the rotor pole pair is measured from the one end of the north-pole magnet to the other end of south-pole magnet combined together.

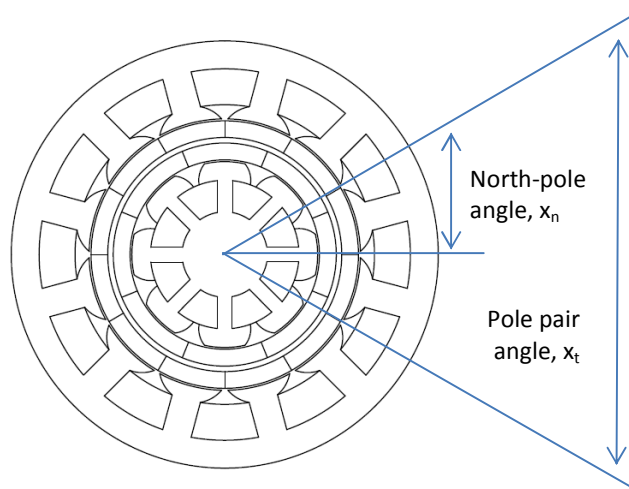


Figure 6.8: Design pole pitch ratio

The default design of the ceiling fan has a pole pitch ratio of 0.5. Four additional variations of design were created by adjusting the North-pole magnet angle while fixing the total pole pair angle. Figure 6.9 shows five variations of different pole pitch ratio as referred to Table 6.3. Each of the variation is then simulated using the Ansoft Maxwell software to obtain the performance result.

Table6.3: Variation of split ratio

Variation	P1	P2	P3	P4	P5
Pole pitch ratio	0.3	0.4	0.5	0.6	0.7
Motor (outer rotor)					
North-pole angle, x_n (°)	18	24	30	36	42
Pole pair angle, x_t (°)	60	60	60	60	60
Generator (inner rotor)					
North-pole angle, x_n (°)	27	36	45	54	63
Pole pair angle, x_t (°)	90	90	90	90	90

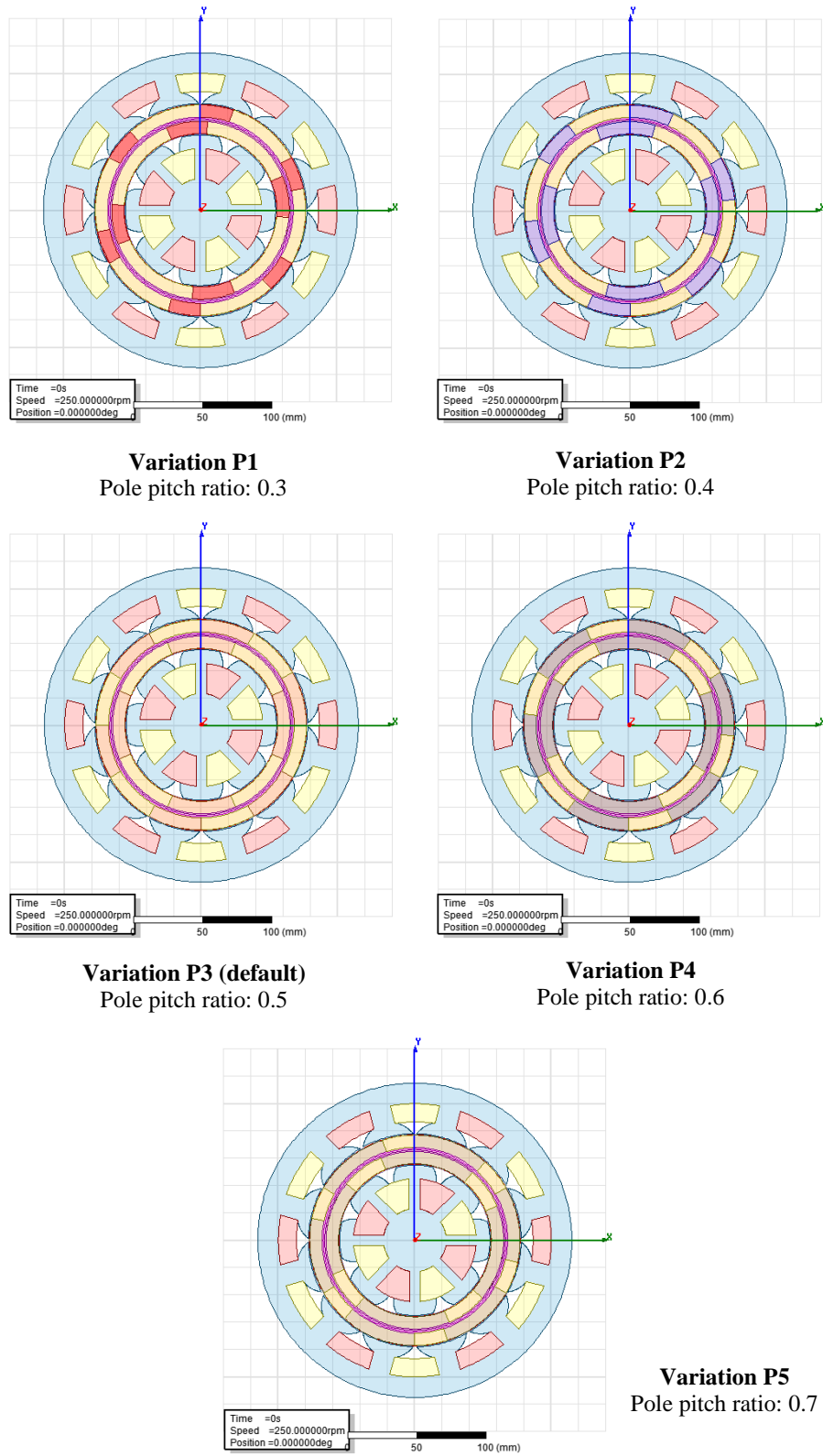


Figure 6.9: Designs with pole pitch ratio variation

6.2.2 Optimisation Result

Similar with the previous split ratio optimisation, the simulation setting and procedure for all five variations is kept to be constant to avoid the possibility of repeatability error resulted from the discrepancy in the design parameter. From the simulation results obtained, the plot for each variation will be layered together to assist observation and comparison procedure. Figure 6.10 and 6.11 show the air gap flux density for both motor and generator of the variation P1, P2, P3, P4 and P5.

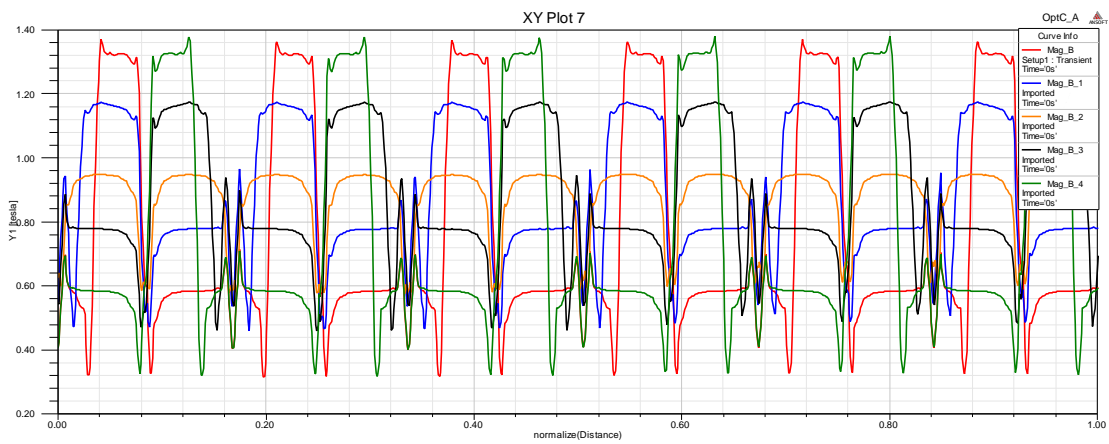


Figure 6.10: Air gap flux density of variation P1, P2, P3, P4 and P5 (motor part)

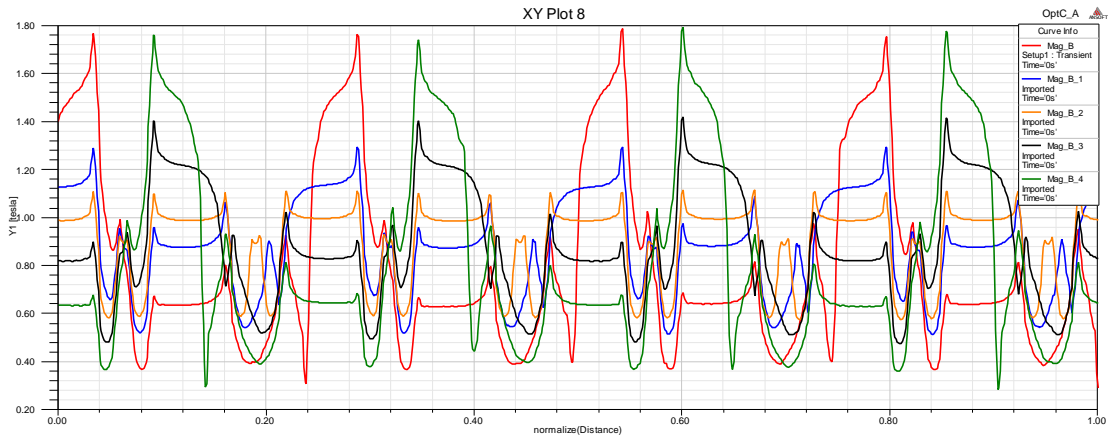


Figure 6.11: Air gap flux density of variation P1, P2, P3, P4 and P5 (generator part)

Both graph plots were being traced at the air gap line between the rotor and stator at the initial position of 0° where the flux flows from the magnet rotor into the stator tooth are at its maximum. The winding coil current is maintained at 0A to avoid flux interference

resulted from current-carrying coil. Each graph contains five plots of air gap flux density denotes by the colour of red, blue, orange, black and green which represent variation P1, P2, P3, P4 and P5 respectively.

Based from the Figure 6.10, variation P2 shows the highest rms value of magnetic flux density at the air gap region of motor part which is approximately 0.89 Tesla followed by variation P4, P3, P1 and P4 in descending order with tiny difference in the value. Same trend had been observed for the air gap flux density of the generator part as shown in Figure 6.11. For the air gap flux density of the generator part, variation P4 produces the highest value with an approximate amount of 0.91 Tesla followed by variation P3, P2, P4 and P1 in descending order with tiny value difference.

The reason behind the negligible difference in the rms value of the air gap flux density is large possibly due to the fixed split ratio where the overall magnet area size and perimeter used for all five variations are kept constant. As the overall area size of the magnet used for the five variations are the same, the total magnetic flux created by the magnet is almost the same in term of their rms value with the only difference in the concentration distribution throughout the magnet air gap region.

Figure 6.12 and 6.13 shows the plots of the induced voltage of different pole pitch ratio design for motor and generator respectively. All five variations produce a similar trend of induced voltage however with different concentration distribution and magnitude.

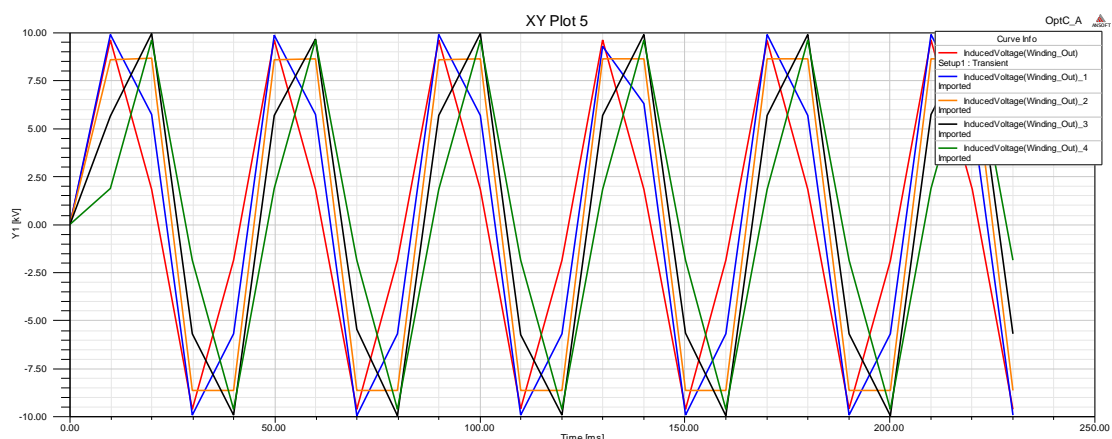


Figure 6.12: Induced voltage of variation P1, P2, P3, P4 and P5 (motor part)

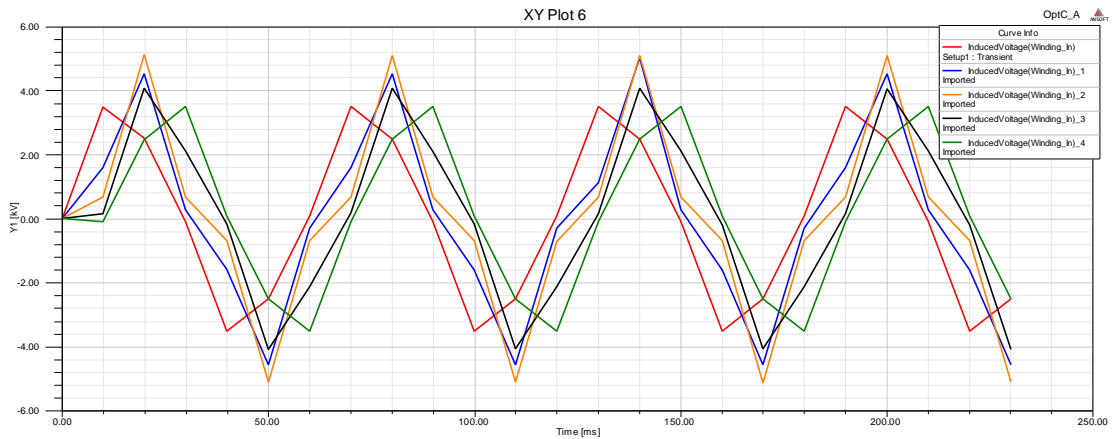


Figure 6.13: Induced voltage of variation P1, P2, P3, P4 and P5 (generator part)

Based on the plot obtained, the rms value of induced voltage for each variation is then tabulated and plotted as shown in Table 6.4 and Figure 6.14.

Table6.4: RMS value of induced voltage (pole pitch ratio)

Variation	P1	P2	P3	P4	P5
Pole pitch ratio	0.3	0.4	0.5	0.6	0.7
Induced voltage (outer winding). V	52.64	59.57	61.88	58.31	50.54
Induced voltage (inner winding). V	17.5	19.53	21.21	18.34	16.73

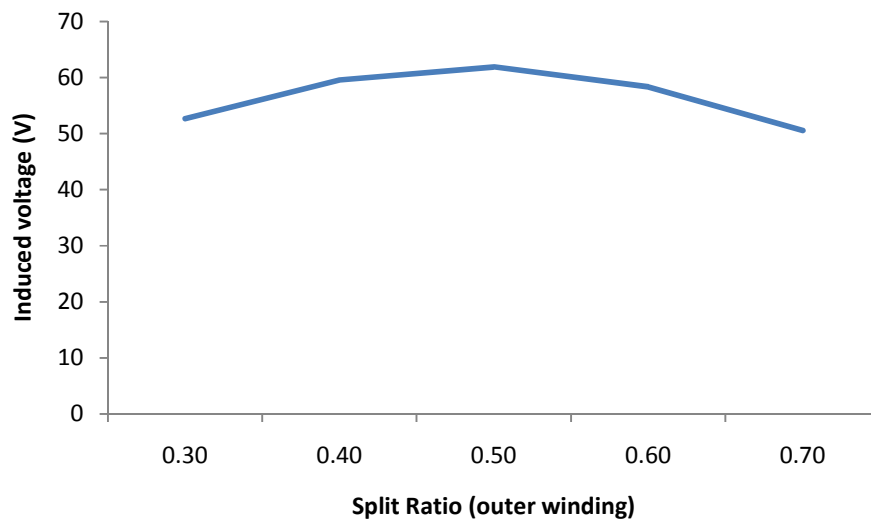


Figure 6.14: Performance plot of pole pitch ratio optimisation

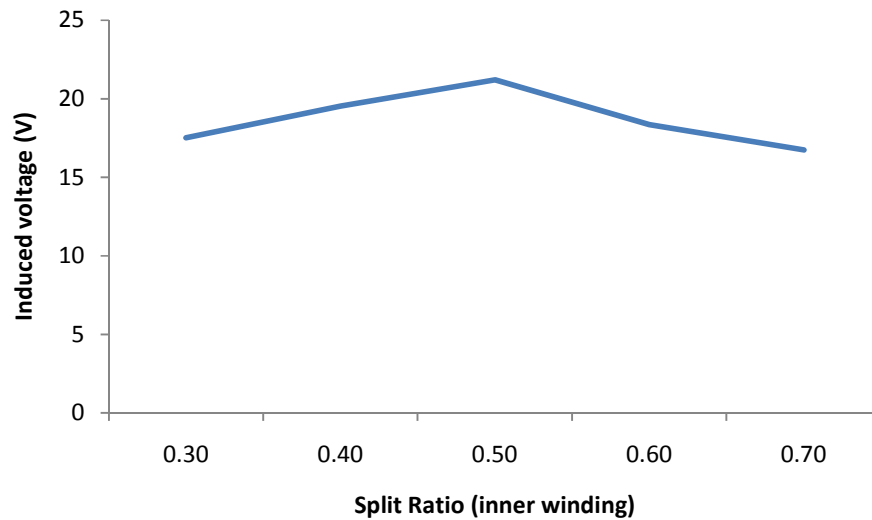


Figure 6.14: Performance plot of pole pitch ratio optimisation (cont.)

From the performance plot shown in Figure 6.14, similar trend of performance plot were identified for both motor and generator part as the ratio of the pole pitch varies. Highest induced voltage value for both parts had been identified at variation P3 with pole pitch ratio of 0.5 where the length ratio between the North-pole and South-pole is equal. The voltage induced by the model is observed to start decreasing as the ratio of the pole pitch increases and decreases away from 0.5.

In another word, the induced voltage of the ceiling fan will decrease as the difference in arc length between the North-pole and South-pole increase. Unbalance ratio between the North-pole and the South-pole of the magnet rotor might cause the discrepancy in the flow of the magnetic flux into the stator thus reducing the amount of the flux being captured by the winding coil thus clarifying the reason of the lower induced voltage. From the result, variation P3 with the pole pitch ratio of 0.5 is selected as the optimised design.

6.3 Conclusion

This chapter discussed the optimisation stage of the selected design models. Two design optimisations had been conducted in order to further optimise the current design; variation of the split ratio and the variation of the pole pitch ratio. The simulation procedure is kept to be constant and the performance for each variation is analysed. Based on the simulation result which focused on the induced voltage of the model, design with the split ratio 0.56 and the pole pitch ratio of 0.50 is selected as the optimised design.

CHAPTER 7

CONCLUSION AND FUTURE WORK

7.0 Conclusion

The primary objective for the project is to propose a novel design of permanent magnet electrical machine for the ceiling fan which can generate electricity. The project is further divided into four sub-objectives that need to be completed in two semesters. All four sub-objectives had been achieved throughout the case study being conducted. The literature studies of various permanent magnet configurations had been conducted in order to minimise the cogging torque problem of the permanent magnet machine as well to obtaining best design configuration for the proposed ceiling fan. Two new designs of novel ceiling fan configuration had been proposed in this paper where the new designs consist of two parts of motor and generator. The motor part of the ceiling fan perform the normal function of ceiling fan while the added generator system will captured the wasted rotating kinetic energy from the moving blade to be converted back into electricity. The proposed designs is simulated to observe and study the flux distribution behaviour of the machine, both rotary stationary as well as the back EMF produced by the machine. The flux distribution behaviour of the simulated model followed the expected flux characteristic. The trend of the back EMF produced showed a good characteristic with the need of adjustment. Two optimisation developments had been conducted to obtain the best performance of the model design; split ratio optimisation and pole pitch ratio optimisation with the optimum ratio of .052 and 0.5 respectively.

7.1 Future Work

The selected design will be further improved and optimised to maximise the performance of the proposed novel ceiling fan machine. The design model also need to be further analysed using the same finite element analysis approaches to obtain and study the power consumption and generation as well as the machine efficiency of the proposed model to be compared with the conventional ceiling fan for the marketing value.

REFERENCES

- [1] "Country Comparison and Historical Annual Data Graph"
<http://www.indexmundi.com>
- [2] Kubota, T., Jeong, S., Toe, D. H. C., Ossen, D. R. (2011) Energy Consumption and Air-conditioning Usage in Residential Building of Malaysia. *Journal of International Development and Cooperation*, Vol.17, No.3, 61-69
- [3] Gieras, J.F. (2010) *Permanent Magnet Motor Technology – 3rd ed.* United States: Taylor & Francis Group
- [4] Chen, S.X.; Low, T.S.; Bruhl, B.; "The robust design approach for reducing cogging torque in permanent magnet motors [for CD-ROM spindles]," *IEEE Transactions on Magnetics*, vol.34, no.4, pp.2135-2137, Jul 1998
- [5] Taeyong Y.; "Magnetically induced vibration in a permanent-magnet brushless DC motor with symmetric pole-slot configuration," *IEEE Transactions on Magnetics*, vol.41, no.6, pp. 2173- 2179, June 2005
- [6] Chen, S.X.; Low, T.S.; Bruhl, B.; , "The robust design approach for reducing cogging torque in permanent magnet motors [for CD-ROM spindles]," *IEEE Transactions on Magnetics* , vol.34, no.4, pp.2135-2137, Jul 1998
- [7] Fazil, M.; Rajagopal, K.R.; , "Development of external rotor single-phase PM BLDC motor based drive for ceiling fan," *Power Electronics, Drives and Energy Systems (PEDES) & 2010 Power India, 2010 Joint International Conference*, vol., no., pp.1-4, 20-23 Dec. 2010
- [8] Yue Zhang; Fengxiang Wang; , "Choice of pole-slot number combination for PM generator direct-driven by wind turbine," *Power System Technology and IEEE Power India Conference, 2008. Joint International Conference on POWERCON 2008*, vol., no., pp.1-4, 12-15 Oct. 2008

- [9] Magnussen, F.; Sadarangani, C.; , "Winding factors and Joule losses of permanent magnet machines with concentrated windings," *Electric Machines and Drives Conference, 2003. IEMDC'03. IEEE International*, vol.1, no., pp. 333- 339 vol.1, 1-4 June 2003
- [10] Ki-Jin Han; Han-Sam Cho; Dong-Hyeok Cho; Hyun-Kyo Jung; , "Optimal core shape design for cogging torque reduction of brushless DC motor using genetic algorithm," *IEEE Transactions on Magnetics* , vol.36, no.4, pp.1927-1931, Jul 2000
- [11] Tae Kyung Chung; Suk Ki Kim; Song-Yop Hahn; , "Optimal pole shape design for the reduction of cogging torque of brushless DC motor using evolution strategy," *IEEE Transactions on Magnetics* , vol.33, no.2, pp.1908-1911, Mar 1997
- [12] Gizaw,D. (1993). U.S. Patent No. 5,250,867. Indianapolis, IN: U.S Patent and Trademark Office
- [13] Jiao, G., Rahn, C.D.; , "Field weakening for radial force reduction in brushless permanent-magnet DC motor," *IEEE Transactions on Magnetics* , vol.40, no.5, pp.3286-3292, Sept 2004
- [14] "ANSYS Software." <http://www.jlrcom.com/ansys-software.htm>